

1 S. Huang, Y. Ye, X. Han, W. Zuo, X. Zhang, L. Jiang 2019. "Performance evaluation of  
2 heating tower heat pump systems over the world." *Energy Conversion and Management*,  
3 186, pp. 500-515. DOI: 10.1016/j.enconman.2019.03.003

## 4 Performance evaluation of heating tower heat pump systems 5 over the world

6 Shifang Huang<sup>a, b</sup>, Yunyang Ye<sup>b</sup>, Xu Han<sup>b</sup>, Wangda Zuo<sup>b</sup>, Xiaosong Zhang<sup>a, \*</sup>, Li Jiang<sup>c</sup>

7 <sup>a</sup> School of Energy and Environment, Southeast University, Nanjing, 210096, PR China

8 <sup>b</sup> Department of Civil, Environmental and Architectural Engineering, University of Colorado Boulder, Boulder, CO 80309, U.S.A.

9 <sup>c</sup> Nanjing TICA Climate Solutions Co., Ltd, Nanjing, 210046, PR China

10 \* Corresponding author. E-mail address: rachpe@seu.edu.cn (Xiaosong Zhang)

11 **Abstract:** Heating tower heat pumps (HTHPs) are proposed as an alternative to the conventional heat pumps. However, lacking  
12 performance evaluation of the HTHPs in different regions limits their applications worldwide. To address this issue, this paper carries  
13 out a large-scale comprehensive performance evaluation of the HTHPs in 869 typical locations. These locations are in the warm, mixed,  
14 and cool climate zones, where buildings need both cooling and heating supply. Seven performance indices are adopted, including the  
15 annual coefficient of performance (COP), COP in cooling season, COP in heating season, regeneration ratio, number of unsatisfactory  
16 hours, matching degree of heat pump, and matching degree of heating tower. The performance evaluation of the HTHPs is conducted  
17 by the processes of location selection, building load calculation, system sizing, simulation, and evaluation. The results show that the  
18 HTHPs have excellent performance in the warm and mixed climate zones, where the average annual COPs are 4.67 and 3.68,  
19 respectively. The HTHPs are also applicable in the cool climate zone with an average annual COP of 3.11. The distributions of all the  
20 performance indices are presented through color maps, and the results are analyzed considering the air temperature and relative  
21 humidity data of the locations.

22 **Key words:** heating tower heat pump; performance evaluation; locations; application; worldwide; coefficient of performance

### 23 1. Introduction

24 Chillers and boilers, air-source heat pumps (ASHPs), and ground-source heat pumps (GSHPs) are widely used  
25 in the regions where buildings need both cooling and heating supply. Chillers have excellent performance in summer,  
26 but they lie idle in winter and boilers are required to satisfy the heating load. However, the boilers can do harm to  
27 the environment. The ASHPs, which can provide both cooling and heating, are becoming the most popular approach  
28 because they can be conveniently installed and maintained. But low efficiency in summer and frosting issue in  
29 winter significantly reduce its annual performance<sup>[1]</sup>. Su et al.<sup>[2]</sup> and Wang et al.<sup>[3]</sup> proposed a novel frost free ASHP,  
30 which adopted liquid desiccant to reduce the humidity ratio of the air flowing through the heat exchangers. However,  
31 this method can increase energy consumption and investment, and the issue of low efficiency in summer remains  
32 unsolved. The GSHPs have high performance in both summer and winter, however, they are subject to topographical  
33 conditions and relatively high initial cost<sup>[4]</sup>. To address these issues, heating tower heat pumps (HTHPs), as novel

1 integrated heating and cooling units, have been proposed as an alternative to the conventional heat pump systems.  
2 The HTHPs have the advantages of high cooling efficiency similar to water chiller and cooling tower systems in  
3 summer. In winter, the HTHPs replace the boilers by using ambient air as a low-potential heat source, which  
4 improves facility utilization ratio and energy efficiency. In addition, the HTHPs address the frosting issue  
5 substantially, and they are easy to install like the ASHPs without the limitation of topographical conditions<sup>[5]</sup>.

6 The previous studies focus more on the mechanism of the components of the HTHP systems, such as heating  
7 towers and regeneration devices. Tan et al.<sup>[6]</sup> made a revision on the Merkel's equation of standard cooling towers  
8 to calculate the thermal characteristics of a heating tower, which is also named as reversibly used water cooling  
9 tower in their study. Fujita et al.<sup>[7][8]</sup> developed a overall enthalpy transfer model for both counter and cross flow  
10 heating towers, and figured out the overall enthalpy transfer coefficients by experiments. Lu et al.<sup>[9]</sup> developed a  
11 coupled heat and mass transfer model for the heating tower. By combining this model and the experimental data,  
12 Wen et al.<sup>[10]</sup> figured out the heat transfer coefficient of a open-type heating tower by assuming Lewis number equal  
13 to one. Then, Huang et al.<sup>[11]</sup> carried out a more detailed experimental investigation and presented the influence of  
14 the inlet air/solution parameters on the performance of the heating tower. In addition, the coupled heat and mass  
15 transfer coefficients were calculated and correlation expressions were developed in this study. Song et al.<sup>[12]</sup>  
16 conducted a similar study on a closed-type heating tower, and compared the results with the heat and mass transfer  
17 process in the liquid desiccant field. Cui et al.<sup>[13][14]</sup> experimentally studied the performance of upward and  
18 downward spraying heating towers, and found they had higher heating efficiency than the ones using gravity  
19 distribution. As for the numerical studies on the performance of heating tower, both Wu et al.<sup>[15]</sup> and Zendejboudi  
20 <sup>[16]</sup> proposed an artificial neural network model. The results in their studies are in good agreement with the  
21 experimental data. Since the heating towers can absorb water vapor from the ambient air, the regeneration devices  
22 are necessary to achieve mass balance. Liang et al.<sup>[17]</sup> and Huang at al.<sup>[18]</sup> found that the heating tower can achieve  
23 self-regeneration in warm and dry working conditions. Huang at al.<sup>[5]</sup> further proposed that the main reason of the  
24 self-regeneration lies in the energy storage characteristic of the solution, and a good amount of regeneration energy  
25 can be saved by taking full advantage of the self-regeneration process. However, the self-regeneration is subjected  
26 to the weather condition. To address this problem, Ai et al.<sup>[19]</sup> proposed a mechanical vapor recompression approach,  
27 and Wen at al.<sup>[20]</sup> investigated a vacuum boiling and condensation approach. Both approaches were found to be more  
28 efficient than the conventional evaporation regeneration approaches because they utilized the condensing heat of  
29 water vapor.

30 The HTHPs have shown advantages over the conventional building cooling and heating systems in some pilot  
31 studies in a few cities. However, their performances have not been systemically evaluated for potential applications  
32 worldwide. Although several experimental studies are related to the system performance (summarized in Table 1),  
33 there are limitations for the evaluations: (1) each study was carried in a specific location in China; (2) there were  
34 huge differences in components and capacities in different studies; (3) the experiments were conducted under only

1 one weather condition or small ranges of temperature and relative humidity; (4) only coefficient of performance in  
 2 heating season,  $COP_h$ , was adopted for evaluation. A large-scale comprehensive performance evaluation of HTHPs  
 3 would help identify their application potential in more regions. However, when conducting such large-scale  
 4 evaluation, the research should meet the following requirements: (1) the locations should be selected over the world;  
 5 (2) the HTHP systems should be designed and sized under the same standard; (3) the HTHP systems should be  
 6 running for a calendar year, which includes both cooling and heating seasons, and consider the part load ratio of the  
 7 systems; (4) the indices should be able to present the performance comprehensively, including the  $COP$  in cooling  
 8 season,  $COP$  in heating season, mean  $COP$  in one year, and regeneration ratio.

9 Table 1. Summary of studies on system performance of HTHPs

Literature	Location	Tower type	Solution	Compressor	Heating capacity	Outdoor weather	$COP_h$
Liang et al. <sup>[21]</sup>	Nanjing	Open-type	Glycol	Rotor	5 kW	$T_a=-2^{\circ}\text{C}$	[2.72, 3.02]
Wu et al. <sup>[22]</sup>	Changsha	Open-type	$\text{CaCl}_2$	Screw	125 kW	$T_a=4.6^{\circ}\text{C}$ , $\phi_a=90\%$	[2.70, 2.86]
Zhang et al. <sup>[23]</sup>	Nanjing	Open-type	Glycol	Rotor	7 kW	$T_a=6.5^{\circ}\text{C}$ , $\phi_a=76\%$	3.02
Li et al. <sup>[24]</sup>	Changsha	Closed-type	Urea	Screw	125 kW	$T_a=[-1, 5]^{\circ}\text{C}$ , $\phi_a=[71\%, 95\%]$	[2.58, 3.90]
Cheng et al. <sup>[25]</sup>	Changsha	Closed-type	/	Scroll	809 kW	$T_a=4.3^{\circ}\text{C}$ , $\phi_a=93.9\%$	3.00
Chen et al. <sup>[26]</sup>	Hangzhou	Open-type	/	Screw	/	$T_a=[-3, 4]^{\circ}\text{C}$	[3.00, 3.73]

10 To address the above problems, this paper carries out a large-scale comprehensive performance evaluation of  
 11 the HTHPs over the world. Firstly, the HTHP model is developed and validated. Then, the performance evaluation  
 12 of the HTHPs is implemented by the processes of location selection, building load calculation, system sizing,  
 13 simulation, and evaluation. Seven performance indices are proposed and adopted to carry out a comprehensive  
 14 evaluation. Finally, all the results are presented through color maps, and the distributions are analyzed by using air  
 15 temperature and relative humidity data of the locations.

## 16 2. System description and modeling

### 17 2.1. Description of HTHP system

18 Fig. 1 demonstrates the schematics of a typical HTHP system, including a heating tower, a heat pump, a  
 19 regeneration device, a solution tank, four pumps, and eight valves. In the cooling season, the HTHP system works  
 20 as a chiller with a cooling tower, with valves 1-4 open and valves 5-8 closed. The evaporator of the heat pump is  
 21 connected with user sides supplying chilled water to the buildings. The condenser of the heat pump is coupled with  
 22 the heating tower, in which water is adopted and evaporates in the tower to reject heat to the ambient air. Make-up  
 23 water is added to this loop to achieve mass balance. The regeneration loop, including the regeneration device,  
 24 solution tank, and solution pumps, is shut down in the cooling season.

1 In the heating mode, valves 5-8 are open, while valves 1-4 are closed. The condenser of the heat pump supplies  
 2 hot water to the building. The evaporator is connected to the heating tower for absorbing heat from the ambient air.  
 3 In this loop, solution with low freezing point (e.g. glycol aqueous, calcium chloride aqueous) is adopted instead of  
 4 water to avoid system freeze. In some conditions, the solution may absorb both heat and mass from the ambient air.  
 5 As a result, the solution becomes diluted, which increases risks of system freeze. To address this problem, a  
 6 regeneration device based on vacuum boiling and condensation is employed to achieve mass balance<sup>[20]</sup>. The  
 7 solution tank is equipped to store dilute solution temporarily in the heating season to make full use of the self-  
 8 regeneration process. Also, it is used for solution storage in the cooling and transition seasons.

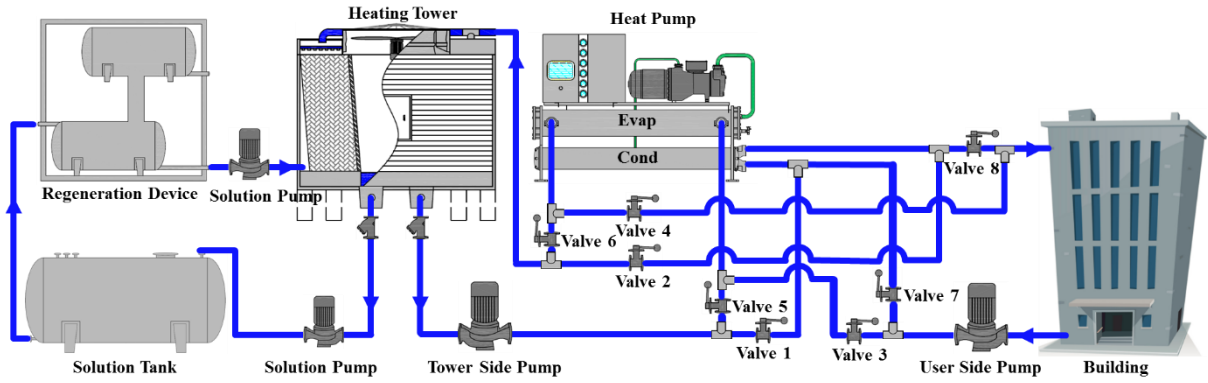


Fig. 1. The schematic of the HTHP system

## 9 2.2. Modeling of HTHP system

10 The models for all the components of the studied HTHP system are developed separately, and then coupled by  
 11 balancing heat, mass and energy between different components. The following sections describe the models for the  
 12 heat pump, heating tower, and regeneration device, respectively.

### 13 2.2.1. Heat pump model

14 The heat pump consists of four main components, including the screw compressor, shell-tube evaporator, shell-  
 15 tube condenser, and thermostatic expansion valve. Models of the components are developed as follows.

#### 16 Compressor

17 The refrigerant mass flow rate,  $M_R$ , and power consumption,  $W_{comp}$ , for screw compressors can be expressed  
 18 by a function of the evaporating temperature,  $T_e$ , and condensing temperature,  $T_c$ <sup>[27]</sup>, and rotation speed  
 19  $N_{comp}$ <sup>[28][29]</sup>:

$$M_R = (\alpha_1 + \alpha_2 T_e + \alpha_3 T_c + \alpha_4 T_e^2 + \alpha_5 T_e T_c + \alpha_6 T_c^2 + \alpha_7 T_e^3 + \alpha_8 T_e^2 T_c + \alpha_9 T_e T_c^2 + \alpha_{10} T_c^3) \frac{N_{comp}}{N_{comp, rated}}, \quad (1)$$

$$W_{comp} = (\beta_1 + \beta_2 T_e + \beta_3 T_c + \beta_4 T_e^2 + \beta_5 T_e T_c + \beta_6 T_c^2 + \beta_7 T_e^3 + \beta_8 T_e^2 T_c + \beta_9 T_e T_c^2 + \beta_{10} T_c^3) \frac{N_{comp}}{N_{comp, rated}}, \quad (2)$$

1 where the subscript *rated* represents the performance under rated speed. The  $\alpha_{1-10}$  and  $\beta_{1-10}$  are coefficients  
 2 regressed from experimental data provided by manufacturer BITZER.

### 3 **Evaporator and condenser**

4 The classical logarithmic mean temperature difference method is adopted in both evaporator and condenser  
 5 models. The cooling capacity of the evaporator,  $Q_e$ , and the heating capacity of the condenser,  $Q_c$ , can be expressed  
 6 as follows:

$$Q_e = K_e A_e LMTD_e , \quad (3)$$

$$Q_c = K_c A_c LMTD_c , \quad (4)$$

7 where  $K$ ,  $A$ , and  $LMTD$  are the heat transfer coefficient, heat transfer area, and logarithmic mean temperature  
 8 difference between refrigerant and water/ solution. The subscript  $e$  represents the evaporator, and  $c$  represents the  
 9 condenser.

10 The overall heat transfer coefficient for the evaporator or condenser,  $K_e$  ( $K_c$ ), can be expressed as a function  
 11 of the heat transfer coefficient inside the tube,  $K_i$ , and outside the tube,  $K_o$ :

$$K_e (K_c) = \frac{1}{\left(\frac{1}{K_i} + R_i\right) \frac{A_o}{A_i} + \frac{\delta A_o}{\lambda_{wall} A_m} + R_o + \frac{1}{K_o}} , \quad (5)$$

12 where  $R$  is the heat transfer resistance. The  $\delta$  is the thickness of the wall. The subscripts  $i$  and  $o$  represent the  
 13 property inside and outside the tube, respectively. And the subscripts  $m$  is the mean value of the inside and outside  
 14 property. The heat transfer coefficients for the evaporation of R22 inside the tube, condensation of R22 outside the  
 15 tube, and water/solution across the tube can be found in our pervious studies<sup>[5]</sup>.

16 The heat transfer capacities of the evaporator and condenser can be expressed by the energy variations of  
 17 refrigerant and water/solution.

$$Q_e = M_R (h_1 - h_4) , \quad (6)$$

$$Q_e = C p_w M_{chw} (T_{chwr} - T_{chws}) \text{ or } Q_e = C p_s M_s (T_{ss} - T_{sr}) , \quad (7)$$

$$Q_c = M_R (h_2 - h_3) , \quad (8)$$

$$Q_c = C p_w M_{cwr} (T_{cwr} - T_{cws}) \text{ or } Q_c = C p_w M_{hw} (T_{hws} - T_{hwr}) , \quad (9)$$

18 where  $h_1$  and  $h_4$  are the enthalpy of the refrigerant in the outlet and inlet of the evaporator,  $h_2$  and  $h_3$  are the  
 19 enthalpy of the refrigerant in the inlet and outlet of the condenser.

### 20 **Expansion valve**

21 The expansion process in the expansion valve is taken as an isenthalpic process as shown in Eq.(10). The mass  
 22 flow rate of the refrigerant can be calculated<sup>[30]</sup>:

$$h_3 = h_4 , \quad (10)$$

$$M_R = C_D A_{th} \sqrt{\rho_{R,l} (P_c - P_e)} , \quad (11)$$

1 where,  $C_D$  is the constant mass flow coefficient. The  $A_{th}$  represents the geometric throat area of the thermostatic  
 2 expansion valve, which is adjustable and controlled by the superheat. The  $P_c$  and  $P_e$  are the pressure of condenser  
 3 and evaporator, respectively.

#### 4 2.2.2. Heating tower model

5 The heating tower model in winter is developed using a finite difference method<sup>[11][18]</sup>. Eqs.(12) and (13)  
 6 express the energy and mass balances between air and solution. Eq.(14) describes the solute balance of the solution.

$$m_a dh_a = -Cp_s m_s dT_s - Cp_s T_s dm_s , \quad (12)$$

$$dm_s = -m_a d\omega_a , \quad (13)$$

$$X_s m_s = (X_s + dX_s)(m_s + dm_s) , \quad (14)$$

7 where  $dh_a$  is the enthalpy variation of the air through an element. The  $dT_s$ ,  $dm_s$  and  $dX_s$  represent the variations  
 8 of the solution in temperature, mass flow rate and concentration through an element, respectively. The  $X_s$  is the  
 9 mass concentration of the solution.

10 The convective heat and mass transfer are also applied as follows:

$$h_c L \cdot dx \cdot dy \cdot \alpha_w (T_s - T_a) = m_a (Cp_a + \omega_a Cp_v) dT_a , \quad (15)$$

$$h_d L \cdot dx \cdot dy \cdot \alpha_w (\omega_s - \omega_a) = m_a d\omega_a , \quad (16)$$

11 where  $\omega_s$  is the equivalent humidity ratio of the solution,  $dT_a$  and  $d\omega_a$  are the temperature and humidity ratio  
 12 variation of air through an element. The  $dx \cdot dy$  represents the size of each element,  $L$  is the length of the packing,  
 13 and  $\alpha_w$  is the specific area of the packing. The  $h_c$  is the heat transfer coefficient,  $h_d$  is the mass transfer  
 14 coefficient. These two coefficients are expressed as functions of the solution mass flow flux,  $G_s$ , and air mass flow  
 15 flux,  $G_a$ :

$$h_c = \gamma_1 G_s^{\gamma_2} G_a^{\gamma_3} , \quad (17)$$

$$h_d = \xi_1 G_s^{\xi_2} G_a^{\xi_3} , \quad (18)$$

16 The coefficients  $\gamma_{1-3}$  and  $\xi_{1-3}$  are regressed from experimental data of our previous study<sup>[11]</sup>.

17 By replacing the subscript  $s$  by  $w$  and setting  $X_s$  to zero, the model listed above can also be used to simulate  
 18 the performance of heating tower in cooling season. The heat and mass transfer capacities in both cooling and  
 19 heating seasons can be expressed as follows:

$$Q_{sh} = (Cp_a + \omega_a Cp_v) \cdot M_a \cdot (T_{a,o} - T_{a,i}) , \quad (19)$$

$$Q_{lh} = r_v \cdot M_a \cdot (\omega_{a,o} - \omega_{a,i}) , \quad (20)$$

20 where  $Q_{sh}$  is the sensible heat transfer capacity, and  $Q_{lh}$  is the latent heat transfer capacity. Here, the positive  
 21 values of  $Q_{sh}$  and  $Q_{lh}$  mean that the heat and mass transfer directions are from air to condenser water or solution.  
 22 When the values are negative, the directions are the opposite. The  $Cp$ ,  $M$ ,  $T$ ,  $\omega$ , and  $r$  represent the specific heat,  
 23 mass flow rate, temperature, humidity ratio, and vaporization latent heat, respectively. The subscripts  $a$ ,  $v$ ,  $i$ , and  
 24  $o$  represent the air, water vapor, tower inlet, and tower outlet, respectively.

### 2.2.3. Regeneration model

A regeneration module based on vacuum boiling and condensation is adopted in this study to satisfy the regeneration demand in winter. The adopted module approximates the efficiency of the regeneration system,  $\eta_{RD}$ , as a constant of 3.4 kg/kWh<sup>[20]</sup>. This is because the performance of this regeneration method is independent of the weather conditions. Then the power input for the regeneration,  $W_{RD}$ , can be calculated by the following equation:

$$W_{RD} = \frac{\int \frac{Q_{th}}{r_w} dt}{\eta_{RD}} \quad (21)$$

### 2.3. Validation of models

The physics-based model developed in this study is validated using our experimental data<sup>[5]</sup>, as shown in Fig. 2. The relative error is within  $\pm 10\%$  for all the predicted values, and the average error is 3.48% for cooling/heating capacity, and 3.05% for the COP. This indicates that the physics-based model has high accuracy in predicting the performance of the HTHP. However, in most experimental runs, the predicted cooling/heating capacity is a little bit higher than the experimental capacity. There are two reasons: 1) In our models, the heat exchangers and pipelines are well adiabatic, while the real system can not reach 100% adiabatic condition. Therefore, there is some heat leakage from the hot water to the surroundings in the winter condition, and some heat absorption from the surroundings to the chilled water in the summer condition. 2) The real system has dirt in the heat exchangers, which can weaken the heat transfer process. Therefore, the experimental cooling/heating capacity can be less than the predicted capacity.

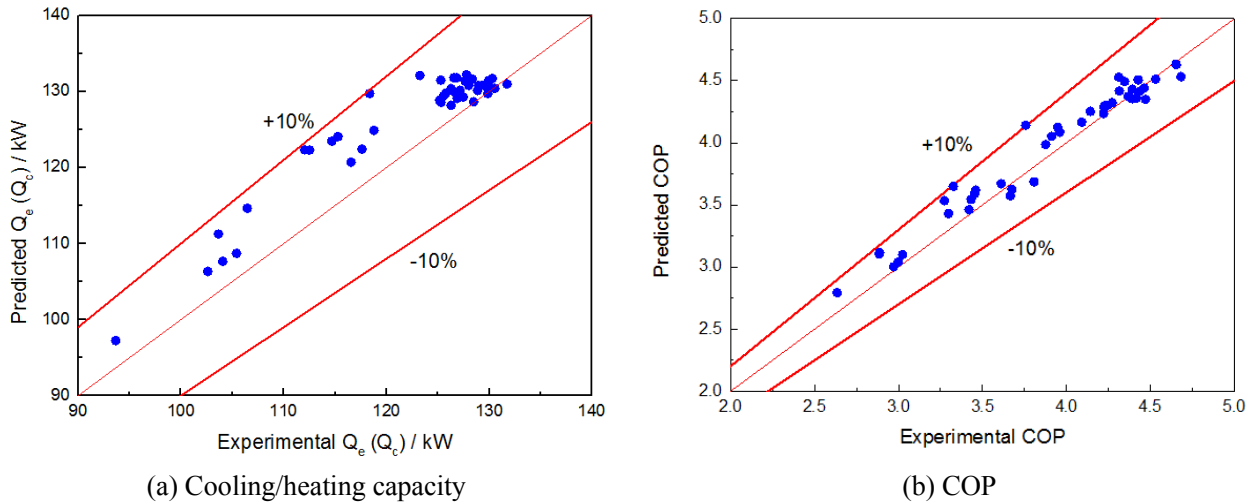


Fig. 2. Comparison between the experimental data and the model prediction of the HTHP

### 3. Performance evaluation of HTHP systems

The performance evaluation of HTHPs over the world is carried out by the steps of location selection, building load calculation, system sizing, simulation, and evaluation, as shown in Fig. 3. The location selection step is to determine the potential thermal climate zones (locations) for HTHPs' application. The building load calculation and

1 system sizing steps are conducted to provide input parameters for system simulations in different locations. In the  
 2 simulation step, hourly simulation for each case is carried out by coupling weather, building, and HTHP system. In  
 3 the evaluation step, seven performance indices are proposed to realize a comprehensive evaluation. The details of  
 4 all the steps will be demonstrated in the following sections.

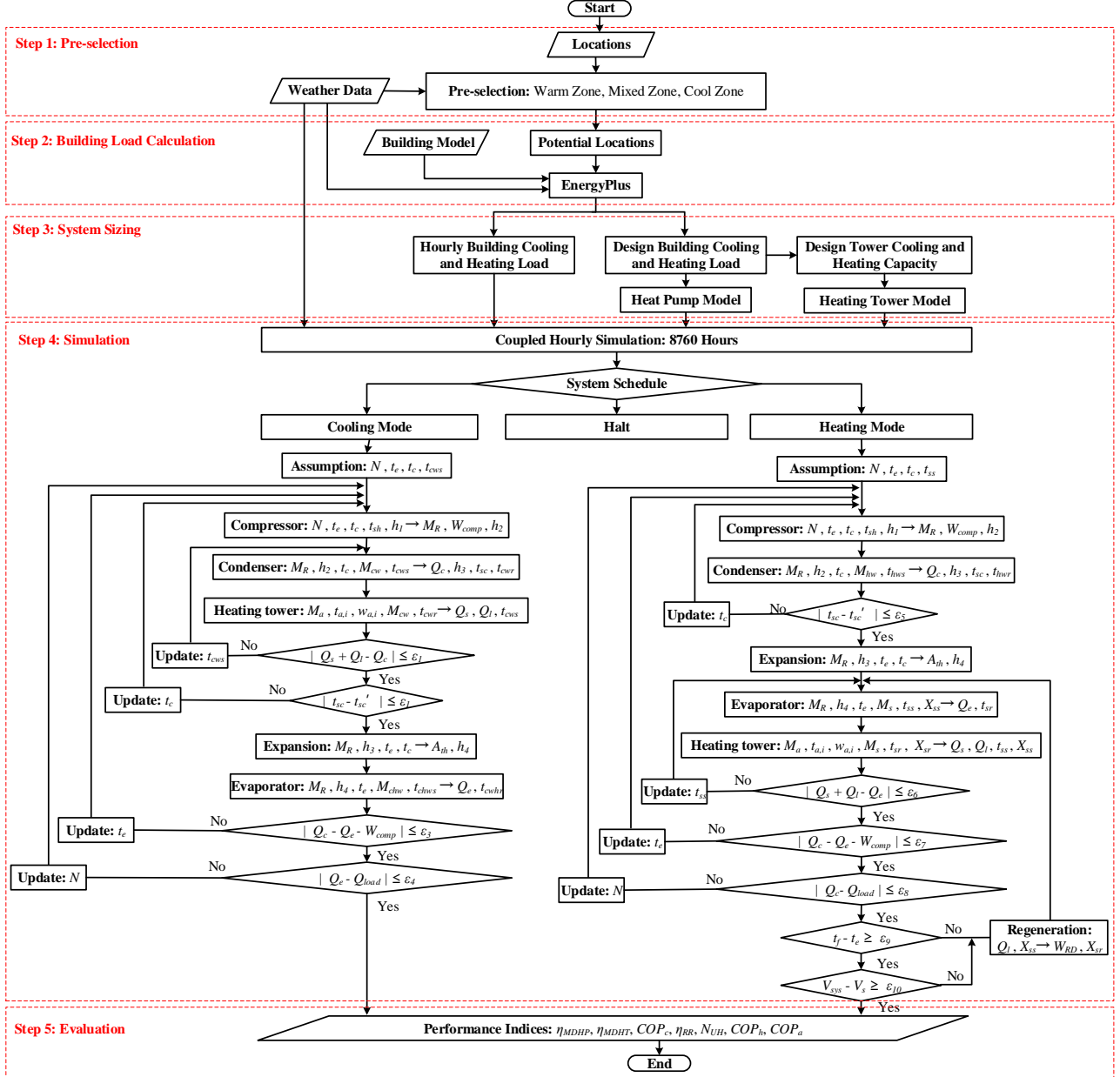


Fig. 3. Flow chart of the performance evaluation of HTHPs over the world

### 3.1. Selection of Locations

The location selection process is carried out first to exclude the regions which are clearly unsuited for the application of the HTHPs. To determine the thermal climate zones for locations over the world, cooling degree-day



1 base 10°C (CDD10°C) and heating degree-day base 18°C (HDD18°C) are adopted, according to ANSI/ASHRAE  
 2 Standard 169-2013<sup>[31]</sup>:

$$\text{CDD10}^\circ\text{C} = \sum_{\text{day}=1}^{365} \max\left(\frac{1}{24} \sum_{\text{hr}=1}^{24} T_a - 10, 0\right), \quad (22)$$

$$\text{HDD18}^\circ\text{C} = \sum_{\text{day}=1}^{365} \max\left(18.3 - \frac{1}{24} \sum_{\text{hr}=1}^{24} T_a, 0\right). \quad (23)$$

3 According to the ranges of the CDD10°C and HDD18°C, nine thermal climate zones are defined, including Zone 0  
 4 (extremely hot), Zone 1 (very hot), Zone 2 (hot), Zone 3 (warm), Zone 4 (mixed), Zone 5 (cool), Zone 6 (cold),  
 5 Zone 7 (very cold), and Zone 8 (subarctic/arctic), as shown in Fig. 4. The buildings in Zones 0-2 only require cooling  
 6 supply, which can be satisfied by chillers. Similarly, boilers are suitable for the buildings in Zones 6-8, which only  
 7 require heating supply, and heat pumps have poor performance in such cold regions. Zones 3-5, where buildings  
 8 need both cooling and heating supply, are considered as the potential regions for the application of HTHPs.

9 Weather data for 2,581 locations is downloaded from EnergyPlus website (<https://energyplus.net/weather>).  
 10 Then, the CDD10°C and HDD18° for all the locations are calculated. After the selection process, 869 locations in  
 11 Zones 3-5 are left, as presented in Fig. 4. Most locations are in China (50, 34, 36 locations in Zones 3-5, respectively),  
 12 the USA (169, 155, 180 locations in Zones 3-5, respectively), and Europe (69, 50, 38 locations in Zones 3-5,  
 13 respectively). The other locations are in the rest of the world (65, 17, 6 locations in Zones 3-5, respectively), such  
 14 as Japan, Australia, and Argentina. The distribution of selected locations is demonstrated in Fig. 5.

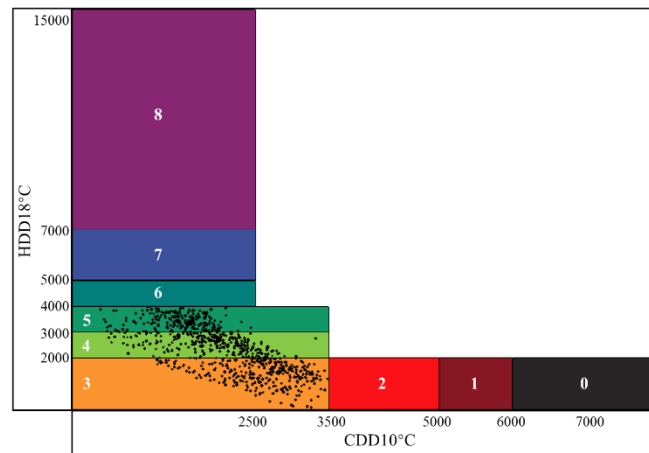


Fig. 4. Thermal climate zones

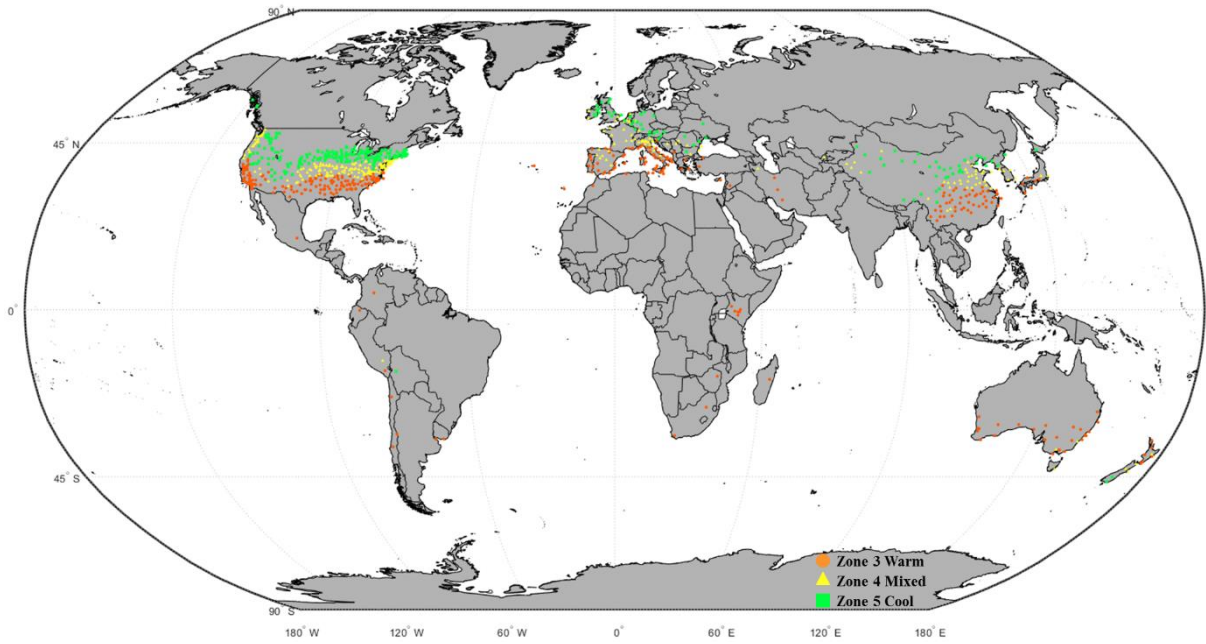


Fig. 5. Distribution of selected locations over the world

### 1 3.2. Building load calculation

2 In the building load calculation process, reference office building models developed by U.S. Department of  
 3 Energy (DOE) are adopted. These reference building models are complete descriptions for whole building energy  
 4 analysis, and organized by climate zones (here, A represents the humid zone, B represents the dry zone, and C  
 5 represents the marine zone<sup>[31]</sup>). The reference buildings have the same shape and architecture, as shown in Fig. 6.  
 6 The details of the settings of envelop, occupancy, and equipment, are demonstrated in Table 2.

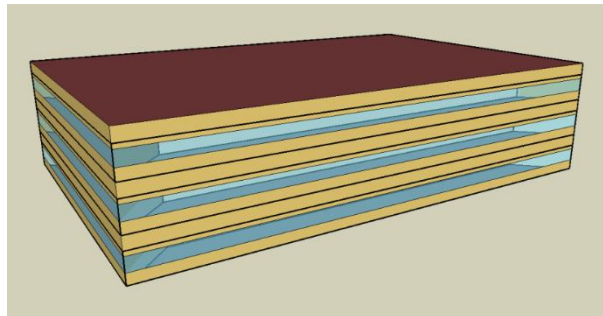


Fig. 6. Building shape and architecture

7 Table 2. Building characteristics in different climate zones

Building characteristics		Climate zones						
		3A	3B	3C	4A	4B	4C	5A
<b>1 General information</b>								
Total floor area	m <sup>2</sup>	4,982						
Cooling indoor set point	°C	24						
Heating indoor set point	°C	21						
Indoor RH	%	60						

<b>2 Building envelope</b>									
R-value of exterior wall	m <sup>2</sup> K W <sup>-1</sup>	1.36	1.10	1.36	1.98	1.76	1.92	2.15	2.15
R-value of roof	m <sup>2</sup> K W <sup>-1</sup>	2.44	3.66	2.00	3.03	2.99	2.75	3.38	3.51
U-value of windows	W m <sup>-2</sup> K <sup>-1</sup>	4.09	5.84	4.09	3.35	4.09	4.09	3.35	3.35
SHGC of windows	/	0.26	0.25	0.39	0.36	0.36	0.39	0.39	0.39
Window-to-wall ratio	/	0.33							
<b>3 Zone summary</b>									
Occupant density	(m <sup>2</sup> person <sup>-1</sup> )	18.58							
Ventilation rate	(l s <sup>-1</sup> person <sup>-1</sup> )	10							
Lighting load	(W m <sup>-2</sup> )	16.90							
Equipment load	(W m <sup>-2</sup> )	10.76							
Infiltration rate	(ACH)	Perimeter: 0.98-1.03; Mid-floor:0.41; Top-floor: 3.76							

1 Based on the reference building models and settings mentioned above, we used Python to call EnergyPlus to  
2 calculate the building loads for the 869 locations. Building loads are used as input data for the system sizing,  
3 simulation, and evaluation, which will be presented in Sections 3.3 to 3.5.

### 4 3.3. Design and sizing of HTHP system

5 A series of heat pumps are designed to satisfy the different building loads of the 869 locations. In the nominal  
6 cooling condition, the supply and return chilled water temperature are 7 and 12°C, and the supply and return cooling  
7 water temperature are 30 and 35°C. In the nominal heating condition, the supply and return solution temperature  
8 are -1 and 1.5°C, and the supply and return hot water temperature are 40 and 45°C. The cooling and heating  
9 capacities,  $COP_c$ , and  $COP_h$  in the nominal cooling and heating conditions are presented in Table 3.

10 Table 3. Parameters of designed heat pumps in nominal conditions

Heat pump type	Cooling capacity	Heating capacity	$COP_c$	$COP_h$
	kW	kW	/	/
HEZEHP080CSH	81	73	4.22	3.39
HEZEHP100CSH	100	92	4.20	3.44
HEZEHP140CSH	135	121	4.28	3.37
HEZEHP160CSH	155	139	4.32	3.40
HEZEHP190CSH	187	171	4.29	3.44
HEZEHP200CSH	203	184	4.38	3.52
HEZEHP210CSH	215	197	4.34	3.46
HEZEHP250CSH	254	230	4.51	3.55
HEZEHP280CSH	281	256	4.43	3.52
HEZEHP320CSH	319	291	4.43	3.52
HEZEHP380CSH	380	343	4.48	3.53
HEZEHP440CSH	440	396	4.58	3.65
HEZEHP510CSH	505	461	4.59	3.66
HEZEHP570CSH	574	523	4.61	3.67

In addition, a series of heating towers are designed to satisfy the different heat rejection and absorption capacities of the heat pumps. In the nominal cooling condition, the air dry/wet-bulb temperature is 32°C/28°C, the air/water flow flux of the heating tower is 2 kg m<sup>-2</sup> s<sup>-1</sup>/4 kg m<sup>-2</sup> s<sup>-1</sup>, and the supply and return cooling water temperature are 30 and 35°C. In the nominal heating condition, the air dry/wet-bulb temperature is 7°C/6°C, the air/water flow flux of the heating tower is the same as that in cooling condition, the supply and return solution temperature are -1 and 1.5°C. In this study, we adopt glycol aqueous as working fluid in heating condition, and its concentration is 15% in the nominal condition. The parameters of the designed heating towers, including heat rejection and absorption capacities, air and water (solution) mass flow rates, are demonstrated in Table 4.

Table 4. Parameters of designed heating towers in nominal conditions

Heating tower type	Heat rejection capacity	Heat absorption capacity	Water/solution flow rate	Air flow rate
	kW	kW	m <sup>3</sup> h <sup>-1</sup>	m <sup>3</sup> h <sup>-1</sup>
HEZEHT130060	132	55	22	24,925
HEZEHT200080	198	82	33	37,388
HEZEHT260110	264	109	44	49,850
HEZEHT330140	330	136	55	62,313
HEZEHT400160	396	164	66	74,776
HEZEHT460190	462	191	77	87,238
HEZEHT530220	528	218	88	99,701
HEZEHT590250	594	246	99	112,164
HEZEHT660270	660	273	110	124,626
HEZEHT730300	726	300	121	137,089
HEZEHT790330	793	328	132	149,551
HEZEHT860360	859	355	143	162,014
HEZEHT930380	925	382	154	174,477
HEZEHT990410	991	409	165	186,939

After the design of the heat pumps and heating towers, the sizing of the HTHPs for different cases can be done with the calculated building loads. Here, we give two examples to show the sizing process. For city Wuhan, China, the designed building cooling/heating load is 411 kW/253 kW, and the corresponding tower heat rejection/absorption load is 500 kW/184 kW. Therefore, heat pump HEZEHP440CSH (440 kW/396 kW) and heating tower HEZEHT530220 (528 kW / 218 kW) are selected to satisfy both cooling and heating demand. For city Beijing, China, the designed building cooling/heating load is 369 kW/297 kW, and the corresponding tower heat rejection/absorption load is 451 kW/213 kW. So, heat pump HEZEHP380CSH (380 kW/343 kW) and heating tower HEZEHT530220 (528 kW / 218 kW) are selected.

### 3.4. Simulation of HTHP system

The weather data, building loads, and system parameters of the selected 869 locations obtained by Steps 1-3 are inputs of Step 4 (simulation). For each location, the simulation of 8,760 hours in one calendar year is carried

1 out, as shown in Fig. 3. According to the building schedule, the modes of the HTHP is selected first, including  
2 cooling, heating, and halt modes. Then, the models of the components mentioned in Section 2.2 are implemented in  
3 the MATLAB environment. To solve the non-linear models which are linked by energy and mass balances, a newton  
4 iterative method is applied. In the cooling mode, the rotation speed of the compressor, evaporating temperature,  
5 condensing temperature, and cooling water supply temperature are selected as iteration variables. The newton  
6 iteration is used to update the iteration variables according to the energy and mass balances between outdoor air,  
7 cooling water, refrigerant, and chilled water. In this paper, the superheating and subcooling values are both set as 5°  
8 C. In the real system, we adjust the geometric throat area of the thermal expansion valve,  $A_{th}$ , to make sure that the  
9 superheating value reaches its set point. But the  $A_{th}$  has a physical constraint, which can only be adjusted from 0%  
10 to the 100% opening. So, we also calculate and record the  $A_{th}$  in the 'Expansion' module. In the most conditions,  
11 the  $A_{th}$  is in the above range since we select appropriate thermostatic expansion valves for all the heat pumps listed  
12 in our manuscript. In some extreme condition when the  $A_{th}$  exceeds the maximum value, we set the  $A_{th}$  as the  
13 maximum value, and then set the superheating value as an unknown. In the heating mode, the cooling water is  
14 replaced by glycol aqueous as the working fluid in the heating tower, and chilled water is replaced by hot water. In  
15 addition, the regeneration device is coupled with the evaporator and heating tower. As mentioned in Section 2.1, the  
16 heating tower absorbs both heat and mass (water) from the ambient air in some conditions. Fortunately, the heating  
17 tower is also able to evaporate the excessive water when the water vapor pressure of the solution is higher than that  
18 of the air<sup>[18]</sup>. This process named as “self-regeneration” can reduce the regeneration load and energy consumption<sup>[5]</sup>.  
19 In order to make full use of the self-regeneration process, the regeneration device only runs when the freezing point  
20 of the solution is not low enough or the volume of the solution is larger than the storage capacity of the system. The  
21 solution with higher concentration has lower freezing point, which can prevent system from freeze and improve the  
22 system safety. However, the increase of concentration can also reduce the water vapor pressure of the solution,  
23 which means that the solution will absorb more latent heat from the ambient air. As a result, the energy consumption  
24 of the regeneration device will increase significantly. So, the ideal state is keeping the safety margin close to 0 °C,  
25 which is the difference between the solution temperature in the outlet of the evaporator and the freezing point of the  
26 solution. In this study, by considering the measuring error and system response time in the real project, we set the  
27 safety margin as 3 °C.

### 28 **3.5. Evaluation of HTHP system**

29 As indicated in the introduction, only  $COP_h$  was adopted for evaluation of HTHP’ operational performance  
30 in heating season in the previous studies. However, more performance indices are required in the designing and  
31 evaluating process of a building’s cooling and heating system. For instance, there are three alternatives for a real  
32 project: chiller and boiler, ASHP, and HTHP. Commonly, we need to compare the initial cost and annual energy  
33 consumption to carry out the economic analysis. Besides the  $COP_h$ , we still need to know the coefficient of  
34 performance of the HTHP in cooling season, the required capacity and energy consumption of the regeneration

1 device. Besides the new newly established system, the HTHP system can also be used to transformation a  
 2 conventional water-cooled chiller system to satisfy both cooling and heating demands. In this case, we need to know  
 3 if additional towers or heat pump hosts are required, which can have an influence on the initial cost. Therefore, we  
 4 propose the matching degree of heat pump and the matching degree of heating tower to address the above problem.  
 5 The detailed definitions and functions of these performance indices are listed as follows.

6 The matching degree of heat pump in cooling and heating modes,  $\eta_{MDHP}$ , is defined as:

$$\eta_{MDHP} = \frac{Q_{DBC}/Q_{DBH}}{Q_{HPC}/Q_{HPH}}, \quad (24)$$

7 where  $Q_{DBC}$  and  $Q_{DBH}$  mean the designed building cooling and heating loads, respectively. The  $Q_{HPC}$  and  $Q_{HPH}$   
 8 are the heat pump cooling and heating capacities, respectively. When  $\eta_{MDHP}$  is larger than 1, it indicates that the  
 9 heat pump should be sized according to the cooling mode in new HTHP system, or no additional heat pumps is  
 10 required in the transformation of a chiller system into a HTHP system. When  $\eta_{MDHP}$  is less than 1, the conclusions  
 11 are the opposite.

12 The matching degree of heating tower in cooling and heating modes,  $\eta_{MDHT}$ , is defined as:

$$\eta_{MDHT} = \frac{(Q_{DBC} + \frac{Q_{DBC}}{COP_{c,rated}}) / (Q_{DBH} - \frac{Q_{DBH}}{COP_{h,rated}})}{Q_{HTC}/Q_{HTH}}, \quad (25)$$

13 where  $COP_{c,rated}$  and  $COP_{h,rated}$  are the rated cooling and heating coefficients of the heat pump, respectively.  
 14 The  $Q_{HTC}$  and  $Q_{HTH}$  are the heating tower cooling and heating capacities, respectively. Similarly, the heating  
 15 tower should be sized to satisfy the tower cooling load in new system, or no additional heating tower is required in  
 16 transformation, when  $\eta_{MDHT}$  is greater than 1.

17 The regeneration ratio in the winter conditions,  $\eta_{RR}$ , is define as follow:

$$\eta_{RR} = \frac{\int Q_{lh} dt}{\int (Q_{lh} + Q_{sh}) dt}. \quad (26)$$

18 The  $\eta_{RR}$  indicates the regeneration penalization in the winter conditions. This performance index can be used to  
 19 size the regeneration device, and to calculate its energy consumption.

20 The number of unsatisfactory hours in the winter conditions,  $N_{UH}$ , is defined as the number of hours when the  
 21 heating capacity of the system cannot satisfy the building heating load:

$$N_{UH} = \int n_{UH} dt, \quad (27)$$

$$n_{UH} = \begin{cases} 1, & Q_{HPH} < Q_{BH} \\ 0, & Q_{HPH} \geq Q_{BH} \end{cases}, \quad (28)$$

$$W_{EH} = \int \max(Q_{BH} - Q_{HPH}, 0) dt, \quad (29)$$

22 where  $Q_{BH}$  represents the building heating load. In the unsatisfactory hours, the unsatisfied heating demands need  
 23 to be provided by an auxiliary electric heater, and  $W_{EH}$  is the power consumption of the electric heater.

24 By considering the energy consumption of heat pump, regeneration device, and electric heater, the energy  
 25 performance of the HTHP is measured by the coefficient of performance,  $COP$ :

$$COP_c = \frac{\int C_{pw} M_{chw} (T_{chw_r} - T_{chws}) dt}{\int W_{HPC} dt}, \quad (30)$$

$$COP_h = \frac{\int C_{pw} M_{hw} (T_{hws} - T_{hwr}) dt}{\int (W_{HPH} + W_{RD} + W_{EH}) dt}, \quad (31)$$







$$COP_a = \frac{\int C_{pw} M_{chw} (T_{chw_r} - T_{chws}) dt + \int C_{pw} M_{hw} (T_{hws} - T_{hwr}) dt}{\int W_{HPC} dt + \int (W_{HPH} + W_{RD} + W_{EH}) dt}, \quad (32)$$

1 where the subscripts  $c$ ,  $h$ ,  $a$  represent cooling season, heating season, and annual, respectively. The  $W_{HPC}$  and  
2  $W_{HPH}$  are heat pump power consumptions in cooling and heating modes, respectively.

### 3 3.6. Development of color map

4 To demonstrate the distributions of all the performance indices for different locations, color maps are developed  
5 by combining the indices and calibrations of the color bars, as shown in Table 5. For instance, Shanghai, China is  
6 selected as the specific location, whose longitude and latitude are 121.47 and 31.40, respectively. The  $COP_a$  of  
7 Shanghai is 4.50, and its [R, G, B] matrix is between [0, 255, 255] and [255, 255, 0]. As the  $COP_a$  increases from  
8 4.0 to 5.0, the R increases from 0 to 255, and the B decreases from 255 to 0 linearly. Therefore, we can obtain the  
9 [R, G, B] matrix by solve the following equations:  $(R+1) / (255+1) = COP_a - 4.0$ ,  $(B+1) / (255+1) = 5.0 - COP_a$ . So,  
10 the [R, G, B] is calculated to be [127, 255, 127]. Similarly, the [R, G, B] matrixes of all the performance indices for  
11 different locations can be obtained, and the color maps are able to be developed based on the results.

12 Table 5. Calibrations of color bars

Color	[R, G, B]	$COP_c$	$\eta_{RR}$	$N_{UH}$	$COP_h$	$COP_a$	$\eta_{MDHP}$	$\eta_{MDHT}$
	[0, 0, 0]	5.0	-35%	-150	2.0	2.0	0.4	0.4
	[0, 0, 255]	5.5	-20%	0	2.5	3.0	0.7	0.6
	[0, 255, 255]	6.0	-5%	150	3.0	4.0	1.0	0.8
	[255, 255, 0]	6.5	10%	300	3.5	5.0	1.3	1.0
	[255, 0, 0]	7.0	25%	450	4.0	6.0	1.6	1.2
	[0, 0, 0]	7.5	40%	600	4.5	7.0	1.9	1.4

## 13 4. Results and discussion

14 According to the steps indicated in Section 3, hourly simulations of the 869 locations are carried out for a  
15 whole year. Based on the results, locations which need cooling or heating supply only for a few days are excluded,  
16 such as locations in Canada, England, south Australia. Seven performance indices for the remaining 762 locations  
17 are calculated, and presented in color map.

### 18 4.1. Performance in cooling season

19 The  $COP_c$  of the HTHPs in cooling season vary from 5.13 to 7.40, as demonstrated in Fig. 7 to Fig. 10. Since  
20 the HTHP works like a water-cooled chiller with a cooling tower in cooling season, the  $COP_c$  is mainly influenced

1 by the air wet-bulb temperature, which is determined the air dry-bulb temperature and relative humidity. As a result,  
2 the locations with lower air dry-bulb temperature or relative humidity have higher  $COP_c$ , such as the ones in  
3 plateaus (Colorado and Utah of the USA, Xinjiang and Gansu province of China) or with maritime climate  
4 (California of the USA, Yunnan province of China, Salamanca of Spain). In general, the  $COP_c$  increases as the  
5 latitude increase because the air dry-bulb temperature usually increases with the latitude. The average  $COP_c$  is 5.73  
6 in Zone 3 (warm), 5.83 in Zone 4 (mixed), and 6.14 in Zone 5 (cool).

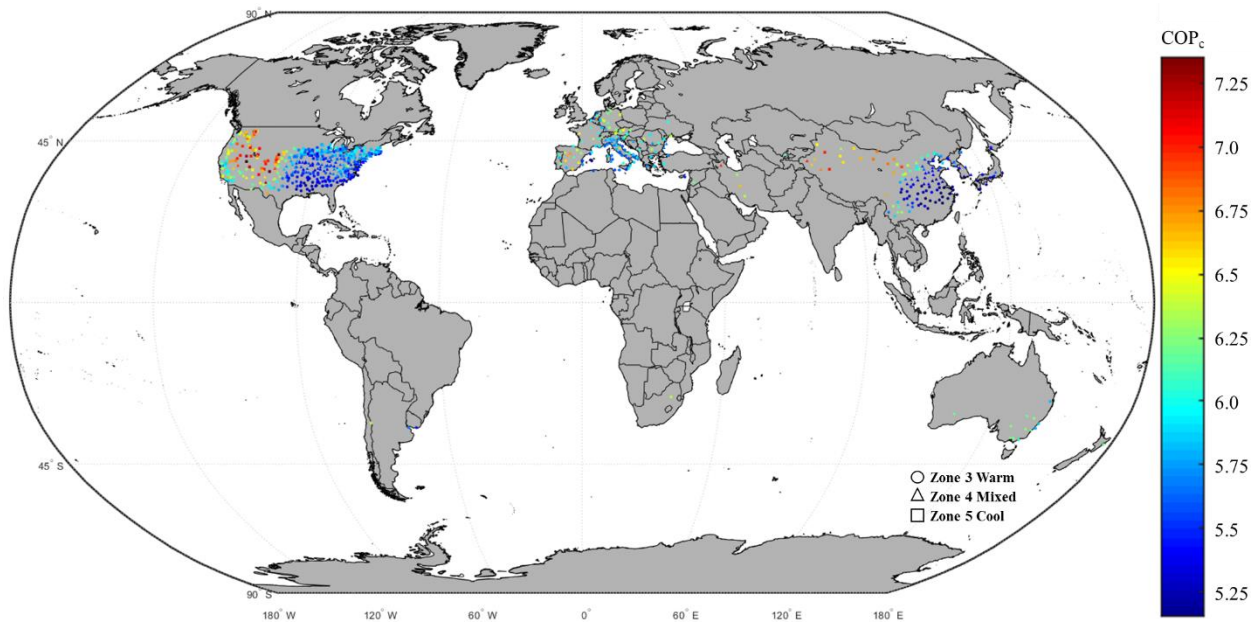


Fig. 7. COP<sub>c</sub> of HTHPs over the world



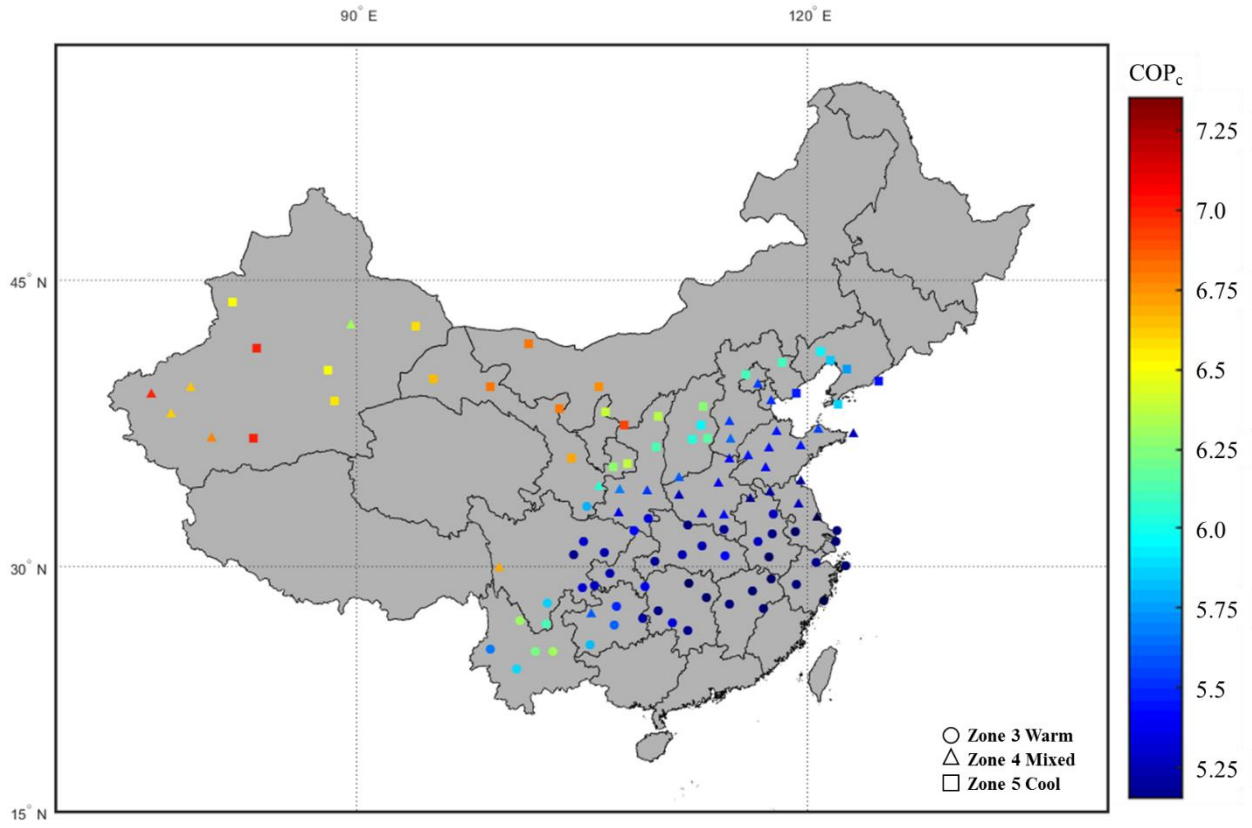


Fig. 8. COP<sub>c</sub> of HTHPs in China

1

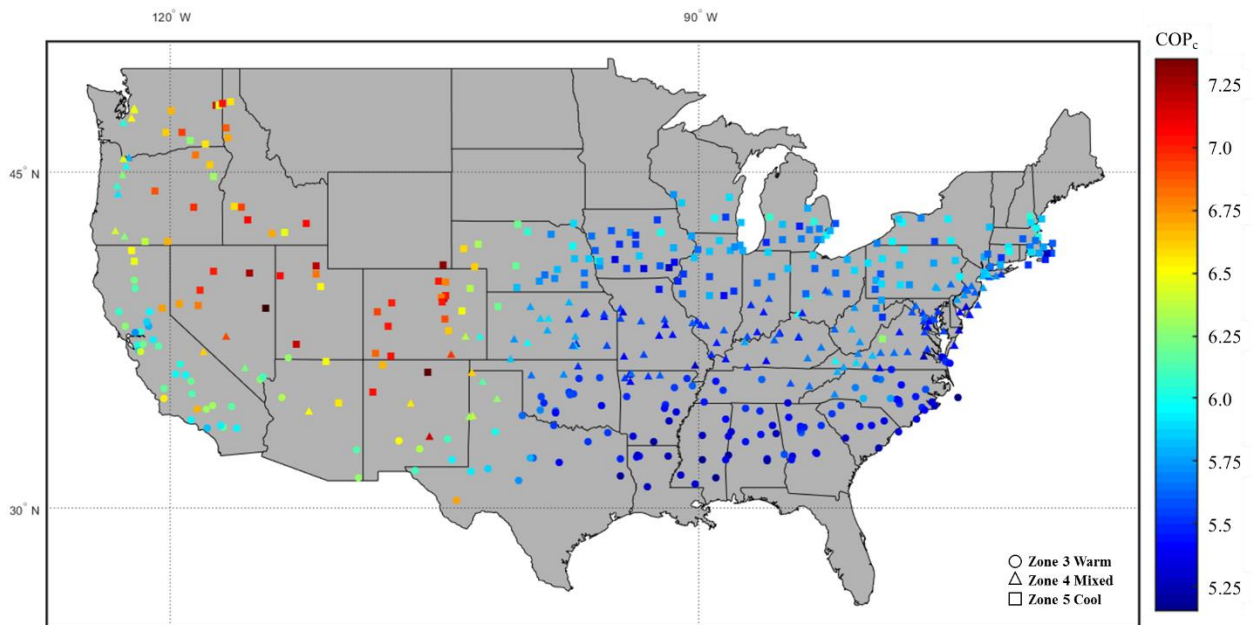


Fig. 9. COP<sub>c</sub> of HTHPs in the USA

2

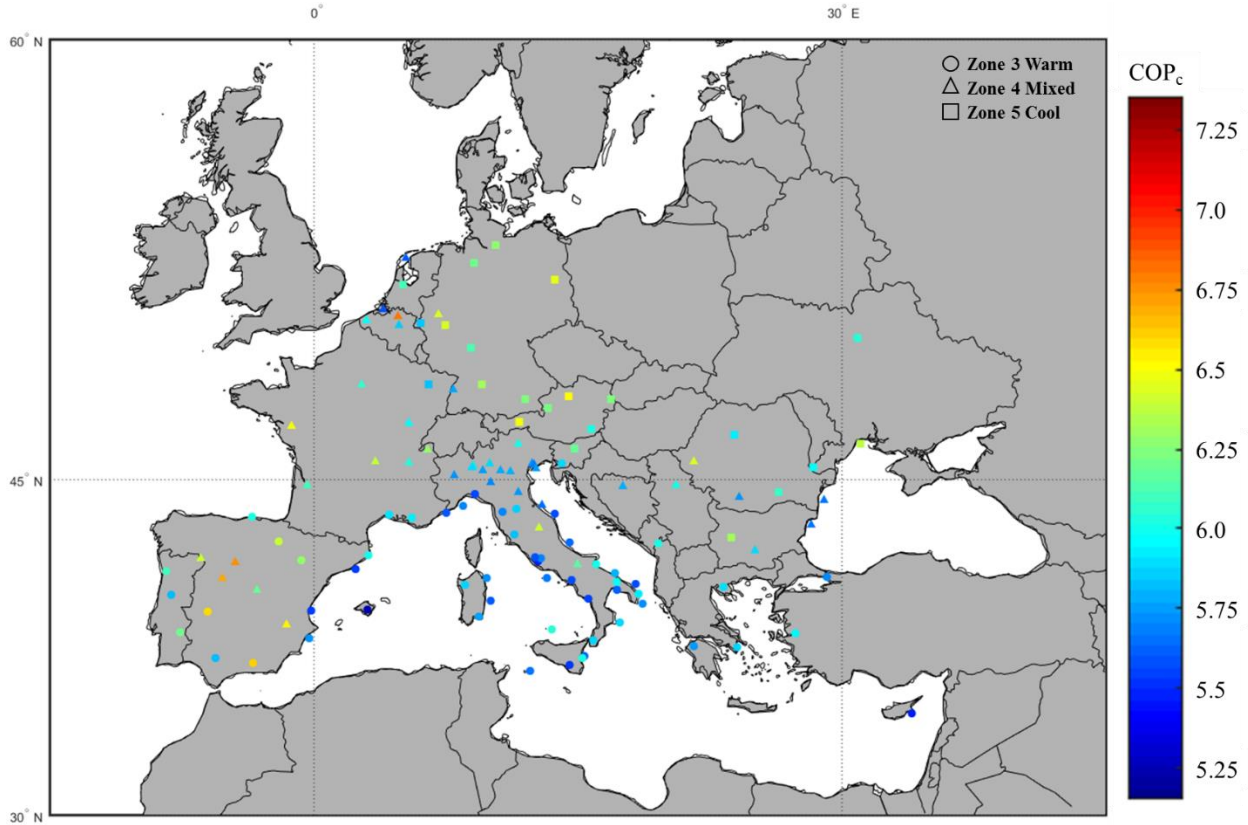


Fig. 10. COP<sub>c</sub> of HTHPs in Europe

#### 1 4.2. Performance in heating season

2 The  $\eta_{RR}$  of the HTHPs which indicates the regeneration penalization (energy consumption of the regeneration  
 3 device) in the heating season, is an important index. The  $\eta_{RR}$  of different locations varies from -33.2% to 34.0%,  
 4 as presented in Fig. 11. When the  $\eta_{RR}$  is larger than zero, it means that the solution absorbs latent heat from the air  
 5 and needs additional energy for solution regeneration. Although the absorbed latent can raise the solution  
 6 temperature, the HTHP costs more electric energy by the regeneration device. In addition, the initial cost also  
 7 increases with larger regeneration capacity. When the  $\eta_{RR}$  is less than zero, it means that the HTHP system can  
 8 achieve the mass balance without addition regeneration. However, the evaporation of water reduces the temperature  
 9 of the solution, which can reduce the efficiency of the system. Therefore, the locations whose  $\eta_{RR}$  is close to zero  
 10 are considered to be better. These locations are marked in light green in Fig. 11, including east-central China, north-  
 11 central of the USA. The mean relative humidity of these locations in heating season are around 70%. The locations  
 12 in southwest China, west coast of the USA, and west Europe, have really high  $\eta_{RR}$ . Since the mean relative humidity  
 13 of these locations in heating season are between 80% and 90%.

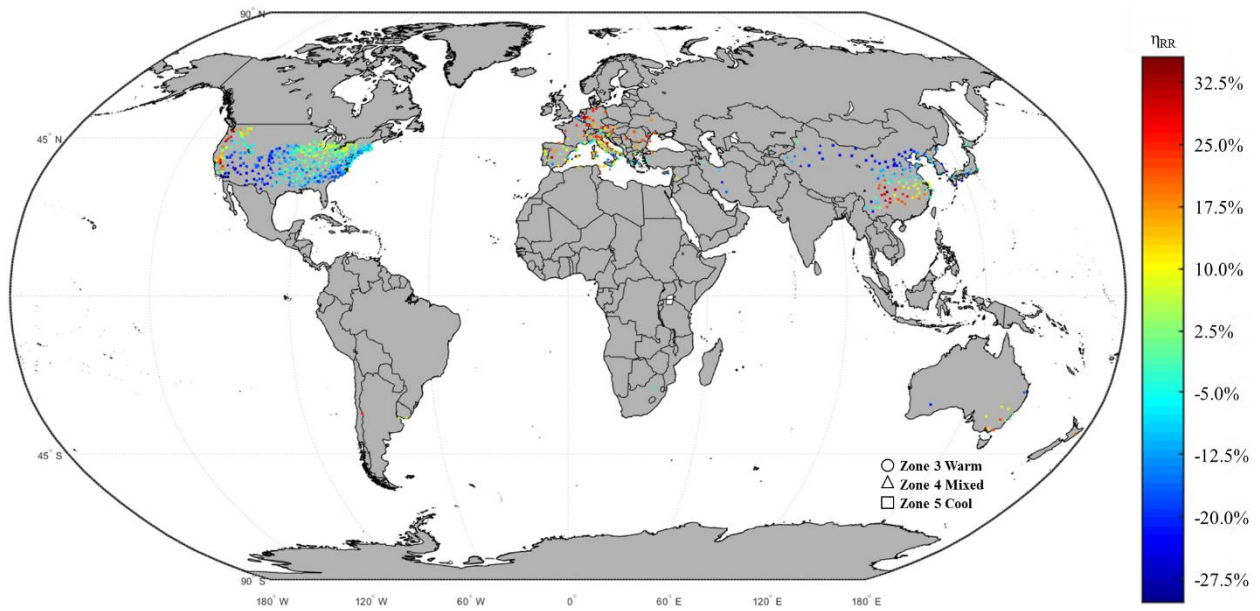


Fig. 11.  $\eta_{RR}$  of HTHPs over the world

1 The  $N_{UH}$  is another important index, which is defined as the number of hours when the heating capacity of  
 2 the system cannot satisfy the building heating load. The higher  $N_{UH}$  means more energy cost by the auxiliary  
 3 electric heater. Due to the energy storage of the solution (absorbing latent heat in the cold and humid hours, and  
 4 self-regeneration in the warm and dry hours), the HTHP shows higher efficiency and capacity than the ASHP under  
 5 severe operating conditions<sup>[5]</sup>. However, the HTHP still has high  $N_{UH}$  when applied in the north China, north-  
 6 central and northeast of the USA, as shown in Fig. 12. Since these regions have really low temperature in the heating  
 7 season. The  $N_{UH}$  of the locations with maritime climate (e.g. California of the USA, Yunnan province of China,  
 8 Salamanca of Spain), is close to zero, since these locations have warm heating season.

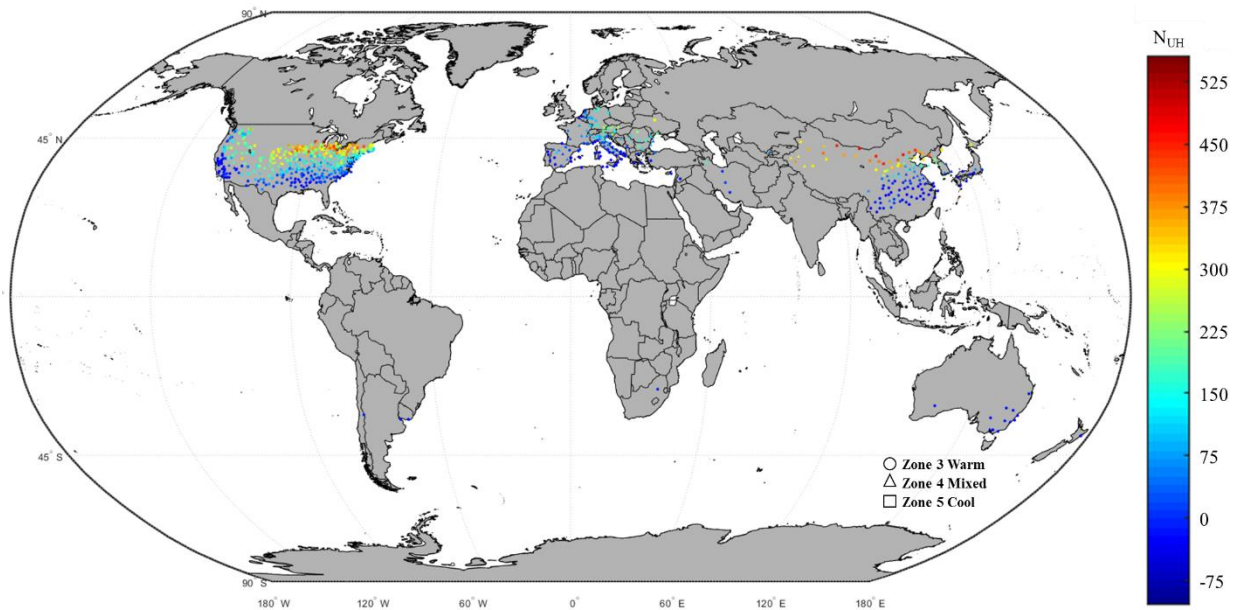


Fig. 12.  $N_{UH}$  of HTHPs over the world

1 The  $COP_h$  taking into account the energy consumption of the heat pump, regeneration device, and auxiliary  
 2 electric heater, is a comprehensive index for evaluation of HTHP's performance in heating season. The  $COP_h$   
 3 of different locations varies from 2.24 to 4.12, as presented in Fig. 13 to Fig. 16. The  $COP_h$  decreases as the latitude  
 4 increases, since the decrease of dry-bulb temperature can reduce the heat pump efficiency and increase  $N_{UH}$ . The  
 5 average  $COP_h$  is 3.37 in Zone 3 (warm), 2.98 in Zone 4 (mixed), and 2.73 in Zone 5 (cool). The relative humidity  
 6 can also have an influence on  $COP_h$  by affecting energy cost of regeneration and heat pump efficiency as well, as  
 7 indicated in the analysis on  $\eta_{RR}$ . For instance, a comparison between Chongqing (HDD18°C is 1103) and Wenzhou  
 8 (HDD18°C is 1106) are presented. These two locations have close latitudes and temperature, while the  $COP_h$  of  
 9 Chongqing (2.83) is much lower than that of Wenzhou (3.72), as presented in Fig. 14. The mean relative humidity  
 10 of Chongqing in heating season (86.4%) is much higher than that of Wenzhou (70.0%). As a result, the  $\eta_{RR}$  of  
 11 Chongqing (34.1%) is much higher than that of Wenzhou (-1.3%), which means more energy consumption of  
 12 regeneration for Chongqing. To present the results more clearly, the  $COP_h$  of locations in the USA are also  
 13 demonstrated in Fig. 15.

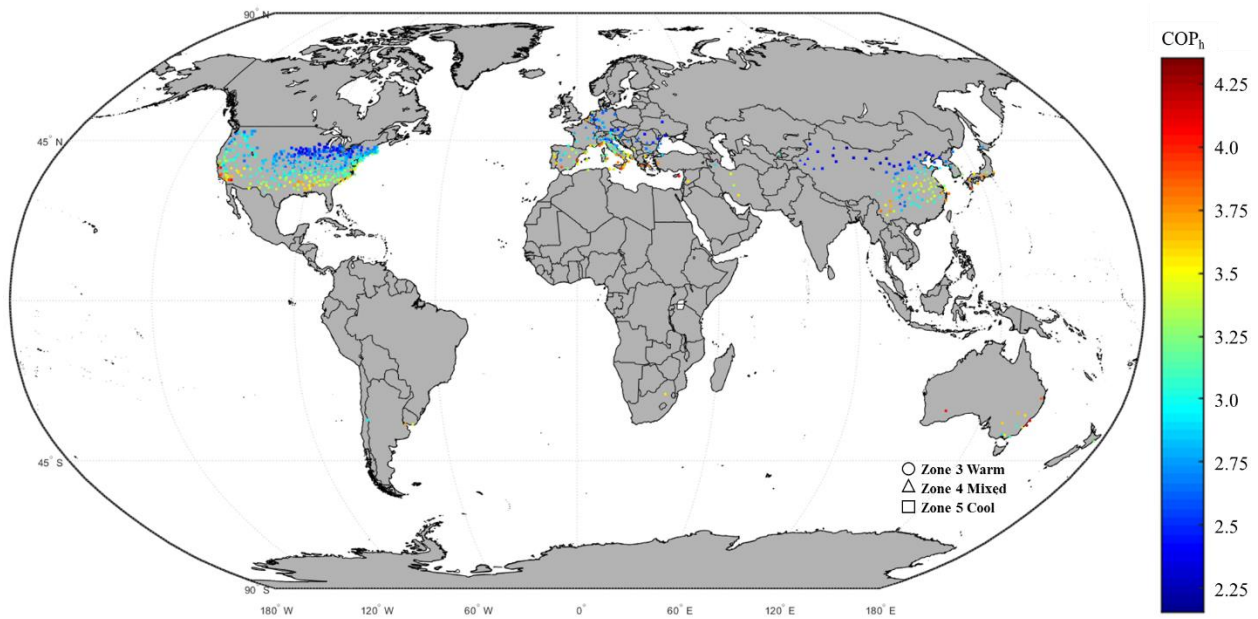


Fig. 13.  $COP_h$  of HTHPs over the world



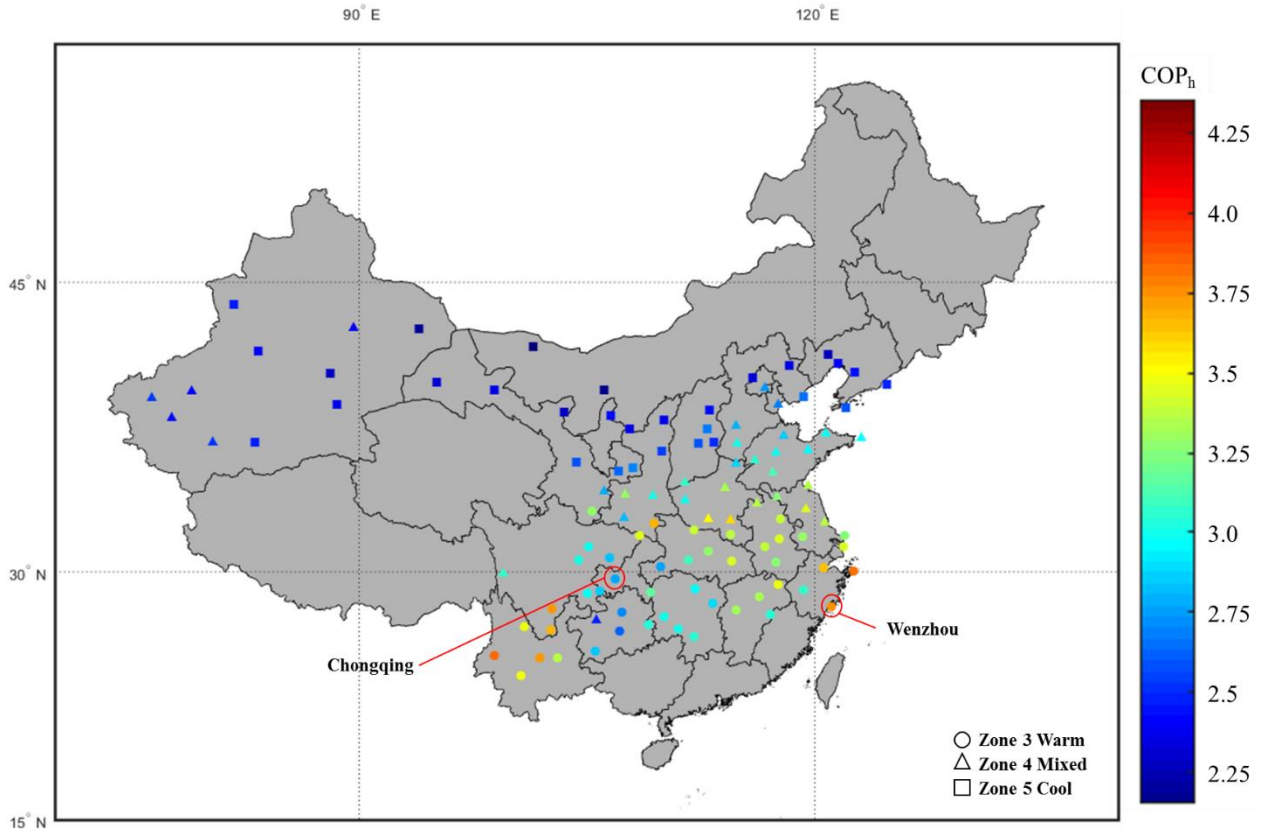


Fig. 14. COP<sub>h</sub> of HTHPs in China

1

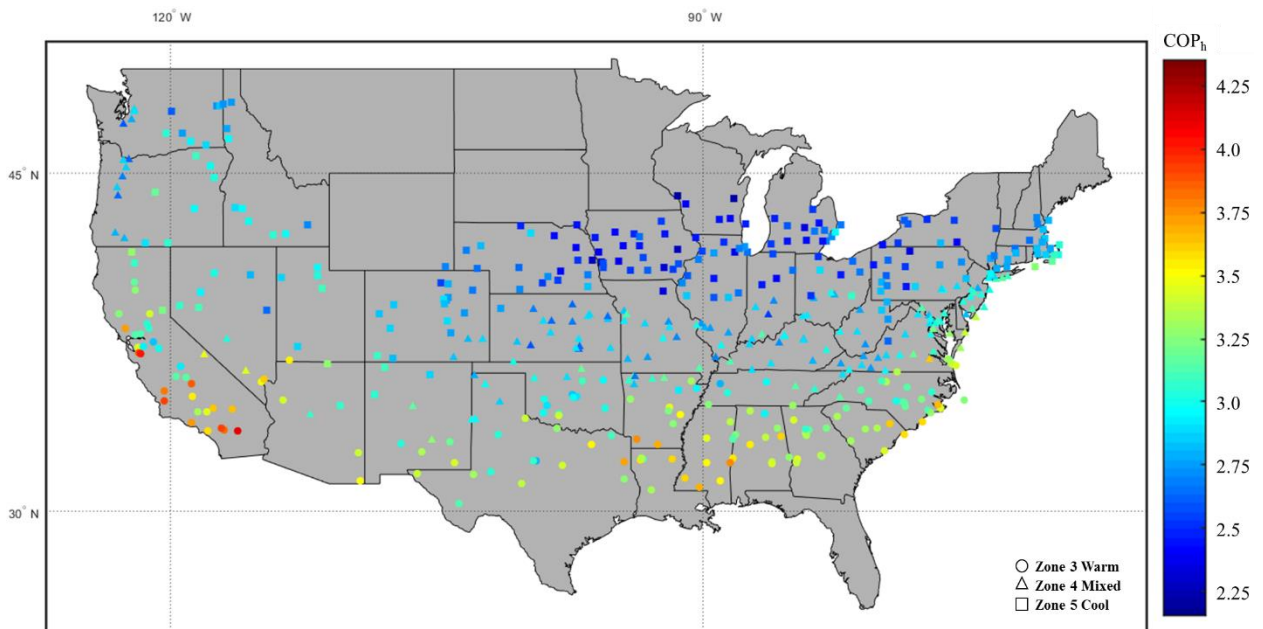


Fig. 15. COP<sub>h</sub> of HTHPs in the USA

2

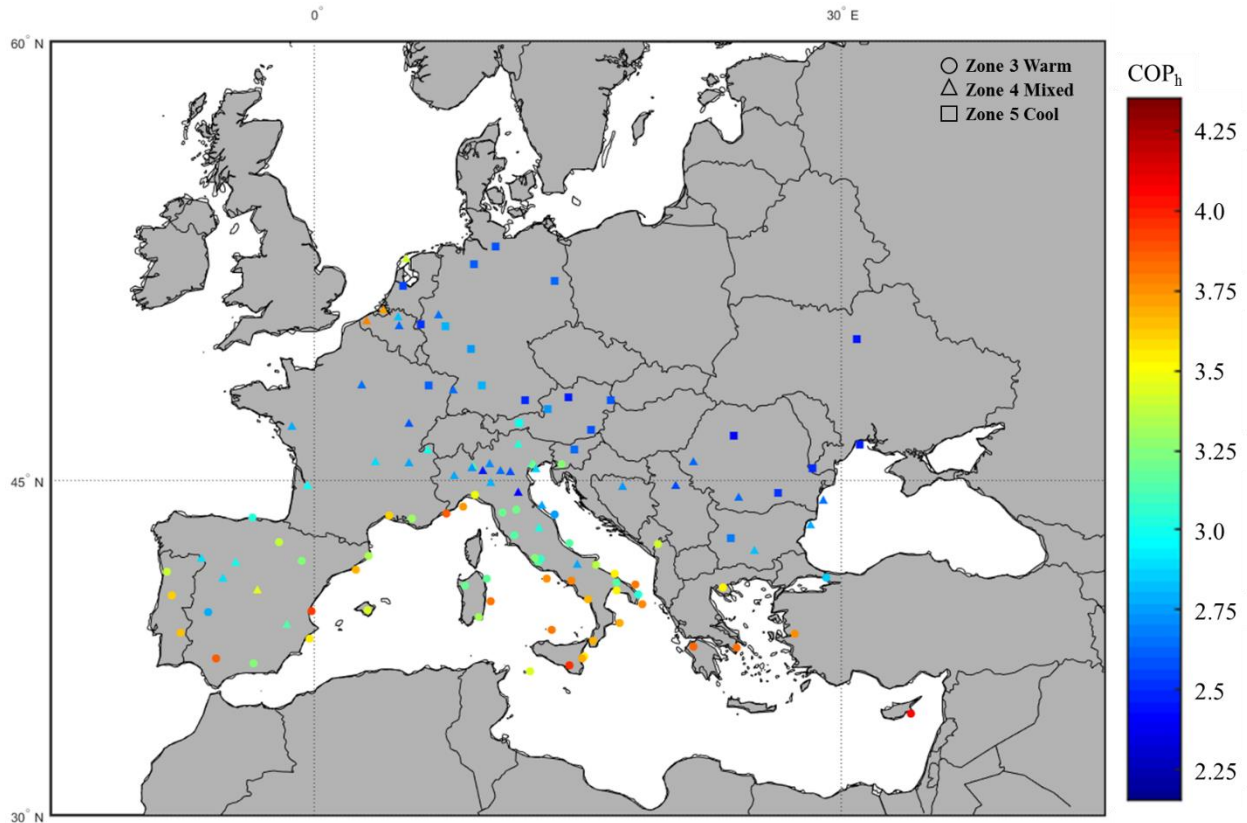


Fig. 16. COP<sub>h</sub> of HTHPs in Europe

### 1 4.3. Annual performance

2 Based on the results and analyses of the HTHP's performance in both cooling and heating seasons, the annual  
 3 performance  $COP_a$  is calculated. Fig. 17 to Fig. 20 present the distributions of the  $COP_a$ , which varies from 2.46  
 4 to 6.10. This index is calculated by taking into consideration of total cooling supply,  $COP_c$ , total heating supply,  
 5 and  $COP_h$ , as indicated in Eq.(32). According to the designed conditions mentioned in Section 3.3, the HTHPs in  
 6 cooling season have lower condensing temperature and higher evaporating temperature than the heating season.  
 7 Therefore, the  $COP_c$  is much higher than the  $COP_h$  as presented in Sections 4.1.1 and 4.1.2. As the latitude  
 8 increases, the total cooling supply decreases and total heating supply increases, which means that the effect of  $COP_c$   
 9 decreases and the effect of  $COP_h$  increases. As a result, the distribution of the  $COP_a$  also follows the variation of  
 10 latitude. The  $COP_a$  of Zones 3 to 5 are 4.67, 3.68, and 3.11, respectively. Specially, the locations with maritime  
 11 climate (e.g. California of the USA, Yunnan province of China, southwest of Europe) has higher  $COP_a$  because  
 12 these locations have cool cooling season and warm heating season.

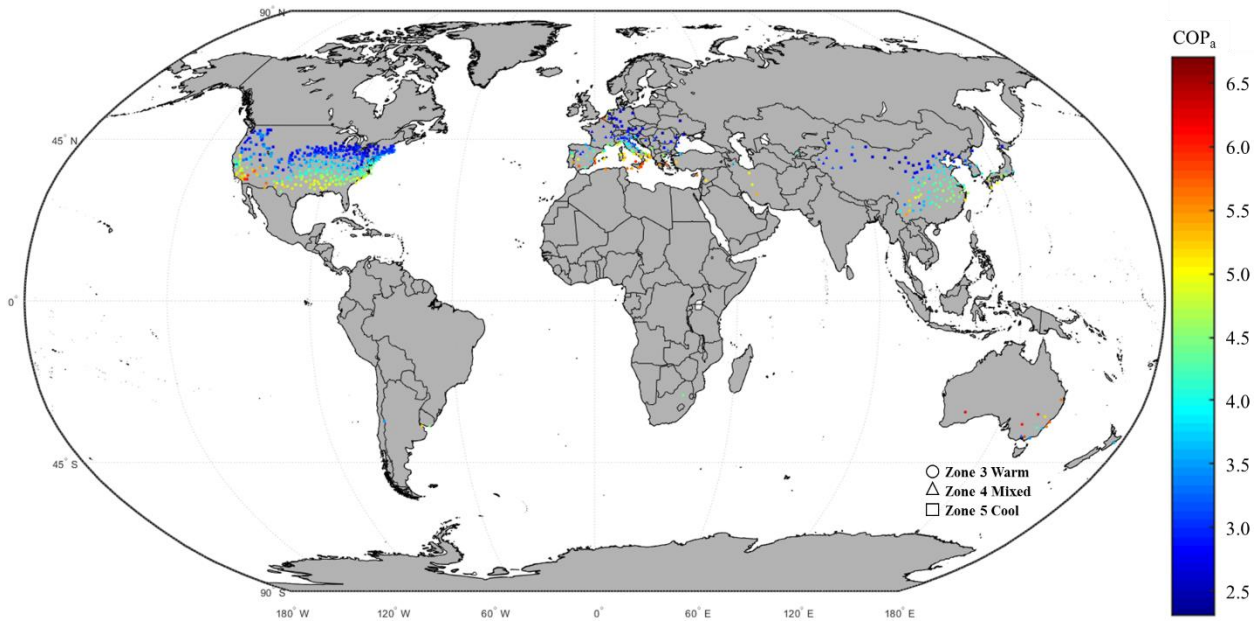


Fig. 17. COP<sub>a</sub> of HTHPs over the world

1

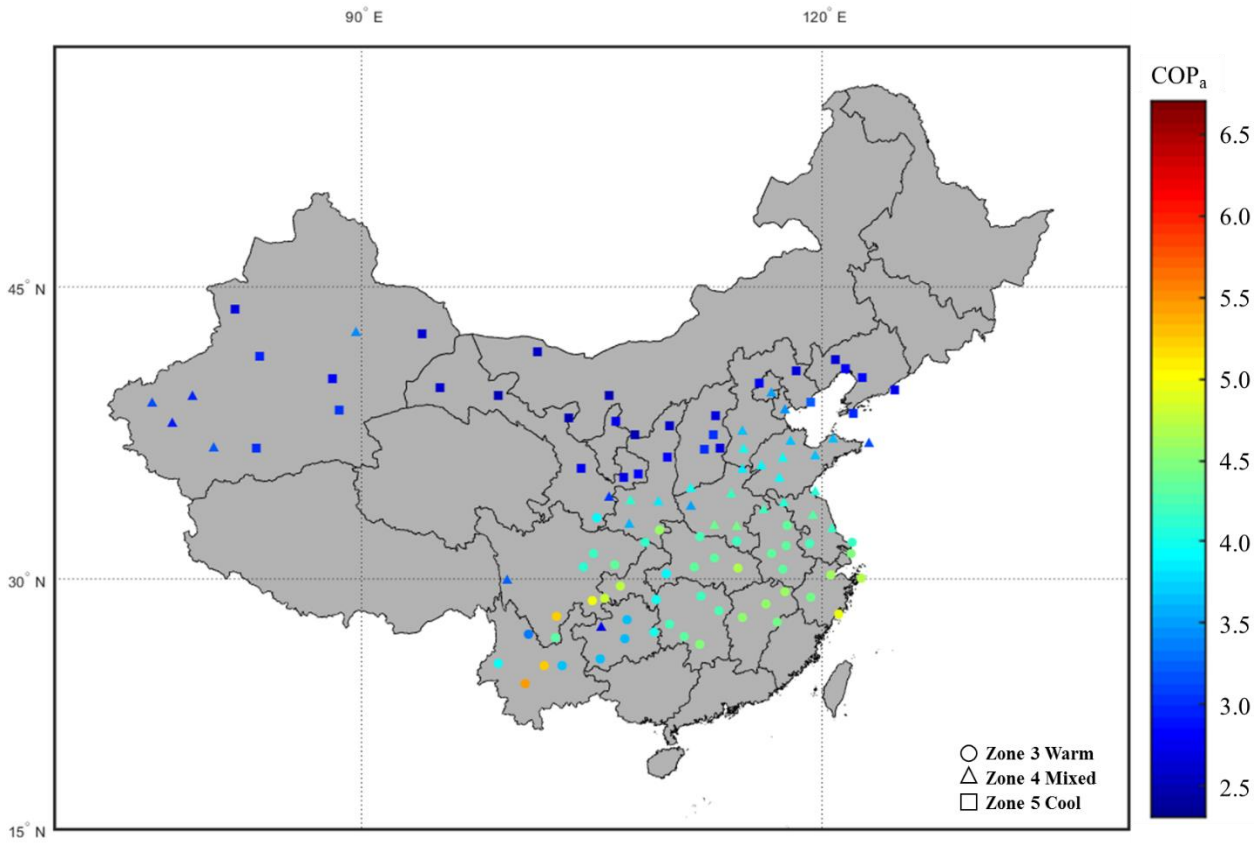


Fig. 18. COP<sub>a</sub> of HTHPs in China

2

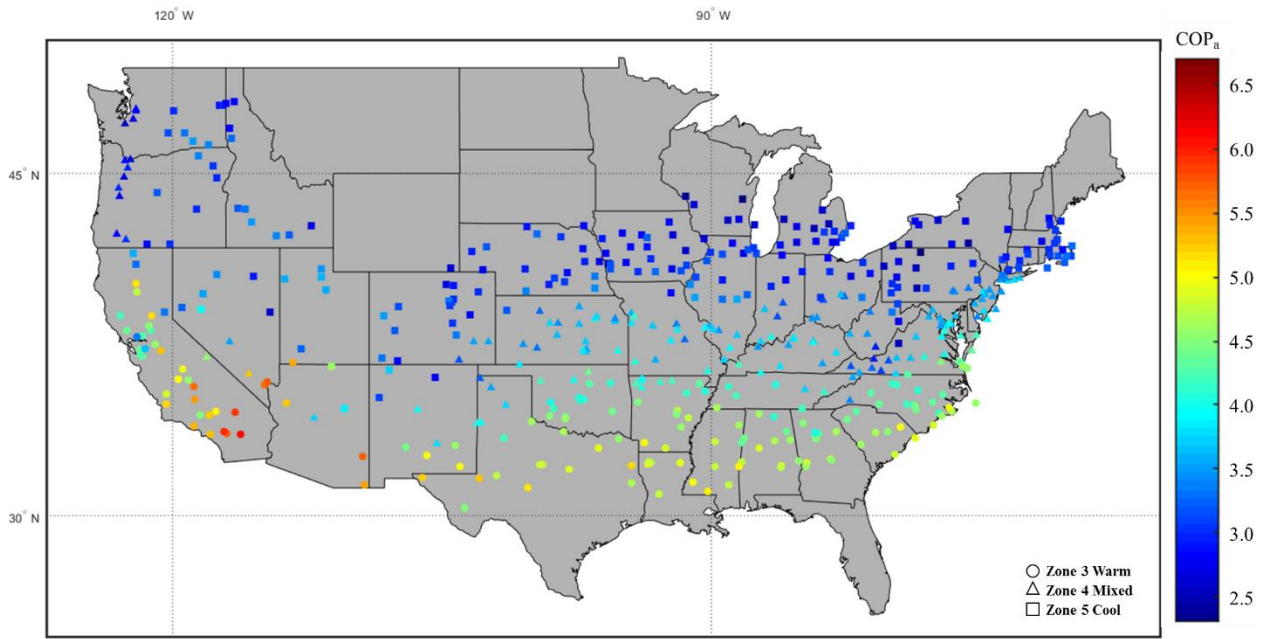


Fig. 19. COP<sub>a</sub> of HTHPs in the USA

1

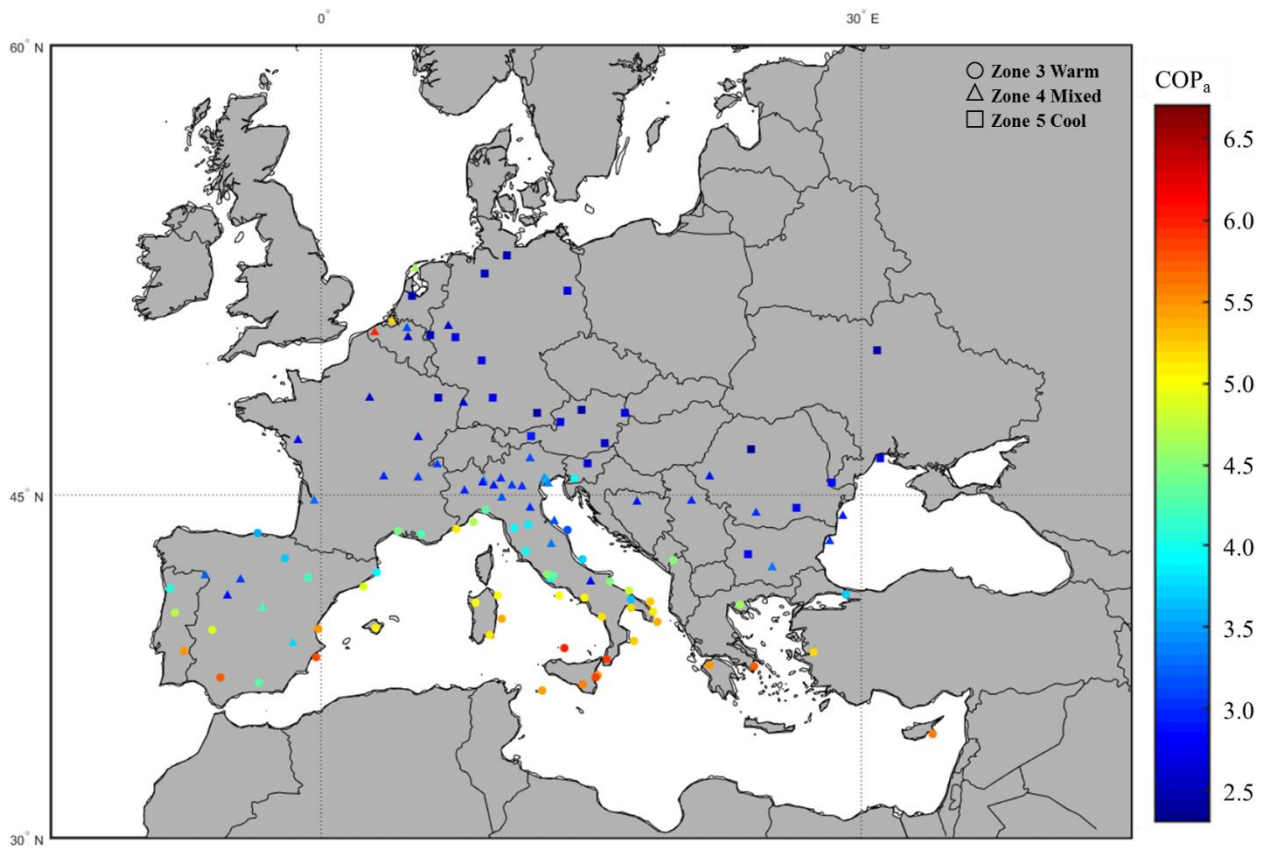


Fig. 20. COP<sub>a</sub> of HTHPs in Europe



1 **4.4. Matching degree of the heat pump and heating tower**

2 The above five indices focus more on the operational performance, while  $\eta_{MDHP}$  and  $\eta_{MDHT}$  can make  
3 contributions in the sizing and transformation process. For traditional heat pumps, such as ASHPs, the  $\eta_{MDHP}$  is  
4 usually larger than 1 in their applications, which means they are designed according to the cooling mode. However,  
5 the  $\eta_{MDHP}$  of the HTHPs has a much larger range when carrying out a large-scale evaluation. The results of  $\eta_{MDHP}$   
6 and  $\eta_{MDHT}$  of different locations are presented in Fig. 21 and Fig. 22, respectively. The  $\eta_{MDHP}$  increases from  
7 0.61 to 1.73 as the latitude increases. The locations with higher elevations (Colorado and Utah of the USA, Xinjiang  
8 and Gansu province of China) or maritime climate (e.g. California of the USA, Yunnan province of China,  
9 Salamanca of Spain) have lower  $\eta_{MDHT}$  than the other locations at the close latitude. When  $\eta_{MDHP}$  is larger than  
10 1, it indicates that the heat pump should be sized according to the cooling mode in new HTHP system, or no add  
11 additional heat pumps is required in the transformation. When  $\eta_{MDHP}$  is less than 1, the conclusions are the  
12 opposite. The  $\eta_{MDHT}$  shows the similar distribution as  $\eta_{MDHP}$ , and the value varies from 0.48 to 1.34, which is  
13 smaller than  $\eta_{MDHP}$  in the same location. This is because the cooling capacity of the heating tower is much larger  
14 than its heating capacity, as indicated in Table 4. Similarly, the heating tower should be sized to satisfy the tower  
15 cooling load in new system, or no additional heating tower is required in transformation, when  $\eta_{MDHT}$  is larger  
16 than 1.

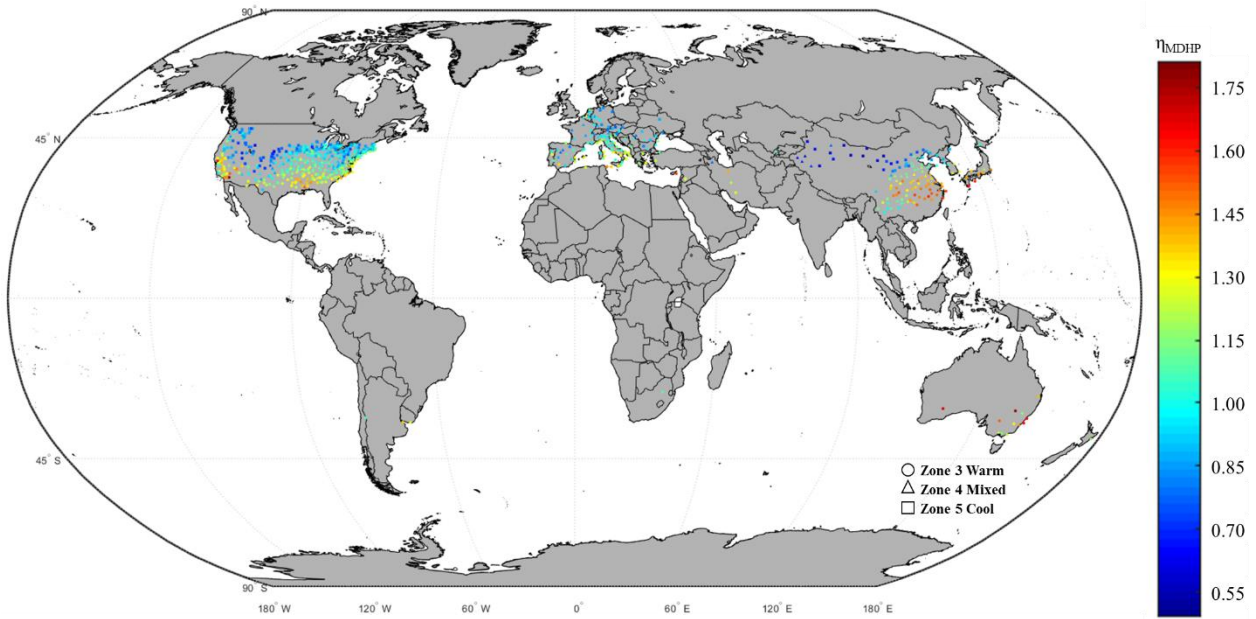


Fig. 21.  $\eta_{MDHP}$  of HTHPs over the world

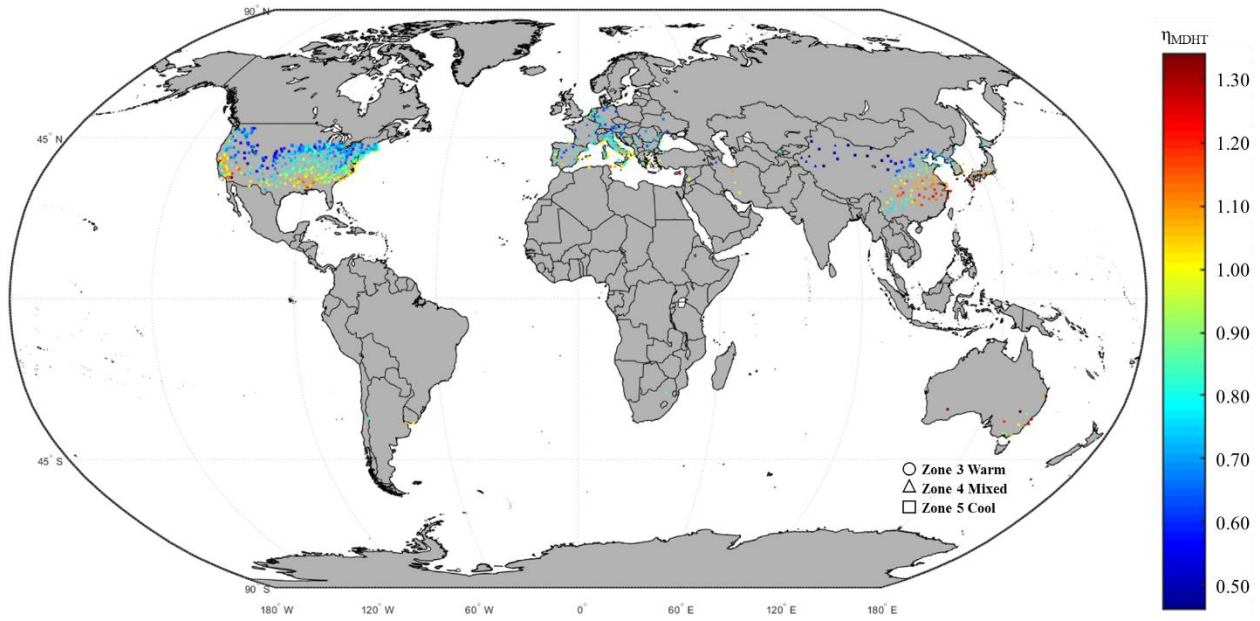


Fig. 22.  $\eta_{MDHT}$  of HTHPs over the world

## 1 5. Conclusion

2 Lacking performance evaluation of the HTHPs in different regions limits their applications worldwide. To  
 3 address this problem, this paper carries out a large-scale comprehensive performance evaluation of the HTHP in  
 4 869 typical locations in the warm, mixed, and cool climate zones. The performance evaluation of the HTHPs is  
 5 implemented by the processes of location selection, building load calculation, system sizing, simulation, and  
 6 evaluation. Seven performance indices are adopted, and presented for all the selected locations. The main  
 7 conclusions are summarized as follows:

8 (1) As the latitude increases, the  $COP_c$  increases from 5.13 to 7.40. The average  $COP_c$  is 5.73 in Zone 3 (warm),  
 9 5.83 in Zone 4 (mixed), and 6.14 in Zone 5 (cool). For the locations with close latitudes, these with high elevations  
 10 or in maritime climate show higher  $COP_c$ .

11 (2) The  $\eta_{RR}$  of different locations varies from -33.2% to 34.0%, and is determined by relative humidity in heating  
 12 season. The  $\eta_{RR}$  is around zero for the locations whose mean relative humidity in winter is about 70%, including  
 13 east-central China and north-central of the USA. The locations whose mean relative humidity in winter is between  
 14 80% and 90% have really high  $\eta_{RR}$ , including southwest China, west coast of the USA, and west Europe.

15 (3) As the latitude increases, the  $COP_h$  of different locations decreases from 4.12 to 2.24. For the locations with  
 16 close latitudes, these with maritime climate or low relative humidity have higher  $COP_h$ .

17 (4) As the latitude increases, the  $COP_a$  decreases from 6.10 to 2.46. The  $COP_{a,s}$  of Zones 3 to 5 are 4.67, 3.68, and  
 18 3.11, respectively. The results indicate that the HTHPs have excellent performance in Zone 3 (warm) and Zone 4  
 19 (mixed), and also can be applied in Zone 5 (cool).

1 (5) As the latitude increases,  $\eta_{MDHP}$  increases from 0.61 to 1.73, and  $\eta_{MDHT}$  increases from 0.48 to 1.34. The  
 2 distributions of these two indices can direct the design of a new HTHP system or transforming of a chiller system  
 3 into a HTHP system.

#### 4 **Acknowledgement**

5 The research described in this paper is supported by the National Natural Science Foundation of China  
 6 (No.51520105009), the China National Key R & D Program (No. 2016YFC0700305), and the Scientific Research  
 7 Foundation of Graduate School of Southeast University (No. YBJJ1708). The research in the US is supported by  
 8 the National Science Foundation (No. IIS-1802017).

#### 9 **Nomenclature**

$A$	heat exchange area, m <sup>2</sup>	$\lambda$	thermal conductivity coefficient, W m <sup>-1</sup> K <sup>-1</sup>
$A_{th}$	geometric throat area of the thermostatic expansion, m <sup>2</sup>	$\zeta$	coefficients of Eq.(18)
$C_D$	constant mass flow coefficient	$\rho$	density, kg m <sup>-3</sup>
$CDD10^\circ C$	cooling degree-day base 10°C, °C	$\omega$	humidity ratio, kg kg <sup>-1</sup>
$COP_a$	annual coefficient of performance, /	<b>Subscript</b>	
$COP_c$	cooling coefficient of performance, /	$a$	air
$COP_h$	heating coefficient of performance, /	$c$	condenser
$C_p$	specific heat capacity, kJ kg <sup>-1</sup> K <sup>-1</sup>	$chws/chwr$	supply / return chilled water
$G$	mass flow flux, kg m <sup>-2</sup> s <sup>-1</sup>	$comp$	compressor
$h$	enthalpy, kJ kg <sup>-1</sup>	$cws/cwr$	supply / return cooling water
$h_c$	heat transfer coefficient of tower, W m <sup>-2</sup> K <sup>-1</sup>	$DBC$	designed building cooling
$h_d$	mass transfer coefficient of tower, g m <sup>-2</sup> s <sup>-1</sup>	$DBH$	designed building heating
$HDD18^\circ C$	heating degree-day base 18°C, °C	$e$	evaporator
$K$	heat exchange coefficient, kW m <sup>-2</sup> °C <sup>-1</sup>	$EH$	electric heater
$L$	length of the packing, m	$HPC$	heat pump cooling
$LMTD$	logarithmic mean temperature difference, °C	$HPH$	heat pump heating
$M$	mass flow rate, kg s <sup>-1</sup>	$HTC$	heating tower cooling
$m$	mass flow rate in one element, kg s <sup>-1</sup>	$HTH$	heating tower heating
$N$	rotation speed, Rev. min <sup>-1</sup>	$hws/hwr$	supply / return hot water
$N_{UH}$	number of unsatisfactory hours, /	$i$	inlet or inner
$P$	pressure, Pa	$l$	liquid phase
$Q$	heat transfer capacity, kW	$lh$	latent heat
$r$	vaporization latent heat, kJ kg <sup>-1</sup>	$m$	mean value of the inside and outside
$R$	Resistance of heat transfer, m <sup>2</sup> K W <sup>-1</sup>	$MDHP$	matching degree of heat pump
$T$	temperature, °C	$MDHT$	matching degree of heat pump
$W$	power consumption, kW	$o$	outlet or external
$X$	mass concentration of solution, /	$R$	refrigerant

<b>Greek symbols</b>		<i>rated</i>	performance under rated speed
$\alpha$	coefficients of Eq.(1)	<i>RD</i>	regeneration device
$\alpha_w$	specific area of the packing, $\text{m}^2 \text{m}^{-3}$	<i>RR</i>	regeneration ratio
$\beta$	coefficients of Eq.(2)	<i>s</i>	solution
$\gamma$	coefficients of Eq.(17)	<i>sh</i>	sensible heat
$\delta$	thickness of the tube wall, m	<i>ss / sr</i>	supply / return solution
$\eta_{MDHP}$	matching degree of heat pump, /	<i>UH</i>	unsatisfactory hour
$\eta_{MDHT}$	matching degree of heat pump, /	<i>v</i>	vaper
$\eta_{RD}$	efficiency of the regeneration system, $\text{kg kWh}^{-1}$	<i>w</i>	water
$\eta_{RR}$	regeneration ratio, /	<i>wall</i>	wall of tube

1

## 2 **References**

- 3 [1] Kim M H, Kim H, Lee K S, et al. Frosting characteristics on hydrophobic and superhydrophobic surfaces: A  
4 review[J]. Energy Conversion and Management, 2017, 138: 1–11.
- 5 [2] Su W, Li W, Zhou J, et al. Experimental investigation on a novel frost-free air source heat pump system combined  
6 with liquid desiccant dehumidification and closed-circuit regeneration[J]. Energy Conversion and Management, 2018,  
7 178(September): 13–25.
- 8 [3] Wang Z, Wang F, Ma Z, et al. Experimental performance analysis and evaluation of a novel frost-free air source heat  
9 pump system[J]. Energy and Buildings, 2018, 175: 69–77.
- 10 [4] Zhang S, Zhang L, Zhang X. Performance evaluation of existed ground source heat pump systems in buildings using  
11 auxiliary energy efficiency index: Cases study in Jiangsu, China[J]. Energy and Buildings, Elsevier B.V., 2017, 147: 90–  
12 100.
- 13 [5] Huang S, Zuo W, Lu H, et al. Performance comparison of a heating tower heat pump and an air-source heat pump:  
14 A comprehensive modeling and simulation study[J]. Energy Conversion and Management, 2019, 180: 1039–1054.
- 15 [6] Tan K, Deng S. A method for evaluating the heat and mass transfer characteristics in a reversibly used water cooling  
16 tower (RUWCT) for heat recovery[J]. International Journal of Refrigeration, 2002, 25(5): 552–561.
- 17 [7] Fujita T, Kawahara K. Thermal characteristics of heating tower part I: Counterflow towers[J]. Transactions of the  
18 Japan Society of Refrigerating and Air Conditioning Engineers, 2012, 6: 265–274.
- 19 [8] Fujita T, Kawahara K. Thermal characteristics of heating towers part II: Crossflow towers[J]. Transactions of the  
20 Japan Society of Refrigerating and Air Conditioning Engineers, 2012, 6: 275–284.
- 21 [9] Lu J, Li W, Li Y, et al. Numerical study on heat and mass transfer characteristics of the counter-flow heat-source  
22 tower (CFHST)[J]. Energy and Buildings, 2017, 145: 318–330.
- 23 [10] Wen X, Liang C, Zhang X. Experimental study on heat transfer coefficient between air and liquid in the cross-flow  
24 heat-source tower[J]. Building and Environment, 2012, 57: 205–213.

- 1 [11] Huang S, Lv Z, Liang C, et al. Experimental study of heat and mass transfer characteristics in a cross-flow heating  
2 tower[J]. *International Journal of Refrigeration*, 2017, 77: 116–127.
- 3 [12] Song P, Wang B, Li X, et al. Experimental research on heat and mass transfer characteristics of cross-flow closed-  
4 type heat-source tower[J]. *Applied Thermal Engineering*, 2018, 135: 289–303.
- 5 [13] Cui H, Li N, Wang X, et al. Optimization of reversibly used cooling tower with downward spraying[J]. *Energy*, 2017,  
6 127: 30–43.
- 7 [14] Cui H, Li N, Peng J, et al. Investigation on the thermal performance of a novel spray tower with upward spraying  
8 and downward gas flow[J]. *Applied Energy*, 2018, 231: 12–21.
- 9 [15] Wu J, Zhang G, Zhang Q, et al. Artificial neural network analysis of the performance characteristics of a reversibly  
10 used cooling tower under cross flow conditions for heat pump heating system in winter[J]. *Energy and Buildings*, 2011,  
11 43(7): 1685–1693.
- 12 [16] Zendehboudi A, Song P, Li X. Performance investigation of the cross-flow closed-type heat-source tower using  
13 experiments and an adaptive neuro-fuzzy inference system model[J]. *Energy and Buildings*, 2019, 183: 340–355.
- 14 [17] Liang C, Wen X, Liu C, et al. Performance analysis and experimental study of heat-source tower solution  
15 regeneration[J]. *Energy Conversion and Management*, 2014, 85: 596–602.
- 16 [18] Huang S, Lv Z, Zhang X, et al. Experimental investigation on heat and mass transfer in heating tower solution  
17 regeneration using packing tower[J]. *Energy and Buildings*, 2018, 164: 77–86.
- 18 [19] Ai S, Wang B, Li X, et al. Numerical analysis on the performance of mechanical vapor recompression system for  
19 strong sodium chloride solution enrichment[J]. *Applied Thermal Engineering*, 2018, 137: 386–394.
- 20 [20] Wen X, Cao X, Yu P, et al. Experimental Research on a Novel Solution Regeneration System for Heat Source tower  
21 Based on Vacuum Boiling and Condensation[J]. *ES Energy & Environment*, 2018, 2: 01–07.
- 22 [21] Liang C, Wen X, Zhang X. Construction and experimental research on heat pump system based on heat-source tower  
23 [J]. *CIESC Journal*, 2010, 61(s2): 142-146.
- 24 [22] Wu J, Zhang G, Zhang Q, et al. Experimental investigation of the performance of a reversibly used cooling tower  
25 heating system using heat pump in winter[J]. *Asia-Pacific Power and Energy Engineering Conference, APPEEC*, 2011,  
26 43: 1685–1693.
- 27 [23] Zhang X, Wen X, Liang C. New type of dual high-efficiency heat pump system suited to hot summer and cold winter  
28 zones [J]. *Refrigeration and air conditioning*, 2013, 13(11): 6-10.
- 29 [24] Li N, Zhang W, Wang L, et al. Experimental study on energy efficiency of heat-source tower heat pump units in  
30 winter condition[C]//*Proceedings - 3rd International Conference on Measuring Technology and Mechatronics Automation*,  
31 *ICMTMA 2011*. 2011, 2: 135–138.
- 32 [25] Cheng J, Zou S, Chen S. Application Research on the Closed-loop Heat-source-Tower Heat Pump Air Conditioning  
33 System in Hot-summer and Cold-winter Zone[J]. *Procedia Engineering*, 2015, 121: 922–929.

- 1 [26] Chen W, Qu L, Wang C, et al. An experimental investigation of the performance of an air-source heat pump hot-  
2 water system based on saltwater energy towers [J]. Journal of Zhejiang University, 2012, 46: 1485-1489.
- 3 [27] Standard A. Performance Rating of Positive Displacement Carbon Dioxide Refrigerant Compressors and  
4 Compressor Units[S]Air-Conditioning, Heating, and Refrigeration Institute, 2013, 571.
- 5 [28] Winandy E, Saavedra C, Lebrun J. Experimental analysis and simplified modelling of a hermetic scroll refrigeration  
6 compressor[J]. Applied Thermal Engineering, 2002, 22: 107–120.
- 7 [29] Park N, Shin J, Chung B. A new dynamic heat pump simulation model with variable speed compressors under  
8 frosting conditions[C]//8th International Conference on Compressors and their Systems. 2013: 681–696.
- 9 [30] Eames I W, Milazzo A, Maidment G G. Modelling thermostatic expansion valves[J]. International Journal of  
10 Refrigeration, 2014, 38(1): 189–197.
- 11 [31] ASHRAE. ANSI/ASHRAE Standard 169-2013 - Climatic Data for Building Design Standards[S]American National  
12 Standards Institute, American Society of Heating, Refrigerating and Air-Conditioning Engineers, 2013: 98.
- 13